

# Implementation of the full CCSDT electronic structure model with tensor decompositions

Michał Lesiuk\*

*Faculty of Chemistry, University of Warsaw, Pasteura 1, 02-093 Warsaw, Poland*

E-mail: lesiuk@tiger.chem.uw.edu.pl

## Abstract

We report a complete implementation of the coupled-cluster method with single, double, and triple excitations (CCSDT) where tensor decompositions are used to reduce its scaling and overall computational costs. For the decomposition of the electron repulsion integrals the standard density fitting (or Cholesky decomposition) format is used. The coupled-cluster single and double amplitudes are treated conventionally, and for the triple amplitudes tensor we employ the Tucker-3 compression formula,  $t_{ijk}^{abc} \approx t_{XYZ} U_{ai}^X U_{bj}^Y U_{ck}^Z$ . The auxiliary quantities  $U_{ai}^X$  come from singular value decomposition (SVD) of an approximate triple amplitudes tensor based on perturbation theory. The efficiency of the proposed method relies on an observation that the dimension of the “compressed” tensor  $t_{XYZ}$  sufficient to deliver a constant relative accuracy of the correlation energy grows only linearly with the size of the system,  $N$ . This fact, combined with proper factorization of the coupled-cluster equations, leads to practically  $N^6$  scaling of the computational costs of the proposed method, as illustrated numerically for linear alkanes with increasing chain length. This constitutes a considerable improvement over the  $N^8$  scaling of the conventional (uncompressed) CCSDT theory. The accuracy of the proposed method is verified by benchmark calculations of total and relative energies for several small molecular systems and comparison with

the exact CCSDT method. The accuracy levels of 1 kJ/mol are easily achievable with reasonable SVD subspace size, and even more demanding levels of accuracy can be reached with a considerable reduction of the computational costs. Extensions of the proposed method to include higher excitations are briefly discussed, along with possible strategies of reducing other residual errors.

# 1 Introduction

Due to numerous favorable properties such as the rigorous size-extensivity, polynomial scaling of the computational costs with the system size and rapid convergence toward the full configuration-interaction (FCI) limit, the coupled cluster (CC) theory<sup>1-6</sup> has become one of the most important theoretical tools for finding approximate solutions of the electronic Schrödinger equation for many-electron atoms and molecules (see Refs. 7,8 for exhaustive recent reviews). In particular, a variant of the CC theory with single and double excitations included in the wavefunction<sup>9,10</sup> and a perturbative treatment of the triple excitations,<sup>11</sup> named CCSD(T), offers a very advantageous accuracy-to-cost ratio and serves as the *gold standard* of computational chemistry. However, in applications where, e.g., accuracy better than 1 kcal/mol is required<sup>12-17</sup> or the wavefunction is no longer dominated by a single reference determinant,<sup>18-23</sup> the CCSD(T) model becomes inadequate. In such cases it is reasonable to climb further up the coupled-cluster ladder and consider the full CCSDT method<sup>24,25</sup> with optional perturbative corrections, akin to (T), to take higher excitations into account.<sup>26-31</sup> Unfortunately, there is a huge gap in the computational costs between the two rungs of the ladder, i.e., with  $N$  being the size of the system, the number of operations needed to calculate the most expensive term in the CCSD(T) equations scales as  $N^7$  while in the CCSDT equations – as  $N^8$ . In practical terms, this translates into orders of magnitude difference in computational timings for realistic systems.

The reasons for this substantial increase of the computational costs are directly linked to the presence of the coupled-cluster triple excitation amplitudes tensor,  $t_{ijk}^{abc}$ , which can no longer be neglected or treated implicitly (details of the notation are given further in the text). The quantity  $t_{ijk}^{abc}$  is treated here as a fully symmetric rank-3 tensor with compound indices  $ai$ ,  $bj$ , and  $ck$ . If one denotes the number of correlated occupied and virtual orbitals by  $O$  and  $V$ , respectively, the dimension of this tensor is  $OV$ . Despite the number of unique elements of the  $t_{ijk}^{abc}$  tensor is very large, roughly  $\frac{1}{6}O^3V^3$ , one can assume that only a comparatively small number of excitations (or linear combinations thereof) is actually

important for the quality of the results. It is thus reasonable to employ rank-reduction or “compression” techniques that decompose the full tensor into quantities of a lower rank, thereby reducing the computational burden and storage requirements of the method. In this paper we rely on the Tucker-3 decomposition<sup>32</sup> which represents the triple excitation amplitudes tensor in the following form

$$t_{ijk}^{abc} \approx t_{XYZ} U_{ai}^X U_{bj}^Y U_{ck}^Z, \quad (1)$$

where the summation over repeating indices is implied, as is throughout the present work. This compression method is successful when the dimension of the tensor  $t_{XYZ}$ , denoted  $N_{\text{SVD}}$  for reasons explained further in the text, is significantly smaller than the initial one,  $OV$ . The first application of the above formula in the coupled-cluster calculations was presented by Hino, Kinoshita and Bartlett<sup>33</sup> at the CCSDT-1<sup>34,35</sup> level of theory (an approximate variant of CCSDT). Despite the results were very promising, a  $N^8$  process was necessary to obtain the  $U_{ai}^X$  tensors, i.e., the method was formally as expensive as the full CCSDT calculations. However, this obstacle has recently been removed<sup>36</sup> and a suitable set of  $U_{ai}^X$  tensors can now be obtained much more cheaply by iterative singular-value decomposition of some approximate  $t_{ijk}^{abc}$  amplitudes. This enables us to apply the decomposition (1) at the CCSDT level of theory which is the main purpose of this work. Let us also stress that the present paper reports the first application of the decomposition (1) in a coupled-cluster method where the triply excited amplitudes must be explicitly formed and stored (in contrast to the CCSDT-1/CC3 methods where the  $t_{ijk}^{abc}$  amplitudes are implicit functions of lower-rank quantities).

It is important to note that various analogues of Eq. (1) have also been employed in the CC calculations for the rank-reduction of the  $T_2$  amplitudes tensor (see Refs. 37,38, 39 and references therein). In particular, in the recent work of Parrish et al.<sup>39</sup> it has been shown that impressive reductions of the computational effort can be obtained if the CCSD

amplitudes are expanded in a set of highest magnitude eigenvectors of the MP2 or MP3 doubles amplitudes. From a mathematical point of view, this idea is very similar to the formalism employed in this work for the  $T_3$  amplitudes based on Eq. (1).

Generally speaking, tensor decomposition methods have a long history in quantum chemistry, although many of them were introduced with help of a different formalism and employing a different language. Most of the effort, until quite recently, has been concentrated on reducing storage requirements and computational effort of handling the electron repulsion integrals (ERI), denoted  $(pq|rs)$  further in the text (Coulomb notation). Probably the most popular method of compressing the ERI tensor is the density fitting (DF) approximation<sup>40–46</sup> (also known as the resolution-of-identity approximation in the present context) where the integrals are expanded into a distinct pre-optimized auxiliary basis set,  $Q$ , as  $(pq|rs) \approx B_{pq}^Q B_{rs}^Q$ . This idea was first proposed in the context of self-consistent field calculations, but since then it has spread to the more advanced electronic structure methods such as MP2 or CC.<sup>47–49</sup> Somewhat later the Cholesky decomposition (CD) of the ERI tensor has been put forward as an important alternative.<sup>50–54</sup> While the decomposition format in CD is effectively the same as in DF, the  $Q$  basis set does not have to be pre-optimized since it is composed of products of the original basis set functions. The main advantage of both CD and DF approximations is that the  $Q$  basis set can be much smaller than the formal rank of the ERI tensor would suggest without an appreciable loss of accuracy. More advanced techniques such as the pseudospectral<sup>55–62</sup> (PS) and chain-of-spheres exchange<sup>63–69</sup> (COSX) methods approximate the ERI tensor in the form  $(pq|rs) \approx X_p^Q Y_q^Q V_{rs}^Q$ , where the  $Q$  summation runs over a set of pre-selected grid points in three-dimensional space. Even more sophisticated ERI decomposition formats have been proposed recently. For example, the tensor hypercontraction (THC) format<sup>70–72</sup> assuming the form  $(pq|rs) \approx X_p^P X_q^P Z_{PQ} X_r^Q X_s^Q$  have been introduced, and Benedikt et al.<sup>38,73</sup> reported representation of the ERI tensor in canonical product (CP) format.

Tensor decompositions can be applied equally well to other quantities appearing in the

electronic structure theory besides the electron repulsion integrals. One important example is the Laplace transformation of the energy denominators that appear in MP and CC theories, introduced first by Almlöf.<sup>74</sup> It has also been realized that tensor decomposition techniques can not only reduce the memory/disk storage requirements and overall computational cost of quantum chemistry methods, but in certain cases they can also decrease their formal scaling with the system size, see Refs.<sup>75–78</sup> as representative examples. However, applications of tensor decomposition techniques to the coupled-cluster amplitudes (at CCSD and higher levels of theory) is a relatively novel development. Starting with the pioneering papers of Kinoshita et al.<sup>37</sup> where the higher-order singular value decomposition (HOSVD) was adopted for compression of  $T_2$  and  $T_3$  amplitudes, several decomposition formats were proposed. Benedikt et al.<sup>38</sup> reported application of canonical product format (also known as parallel factor decomposition) to the  $T_2$  amplitudes at the CCD level of theory, resulting in a substantial scaling reduction down to  $N^5$ . Quite recently the tensor hypercontraction (THC) representation has been applied to the CCSD amplitudes<sup>79,80</sup> and it has been demonstrated that this reduces the scaling of CCSD iterations to  $N^4$ . Finally, we point out that many other techniques that have been used in the literature to reduce the cost of the electronic structure computations can be analyzed and compared more systematically if understood as specific tensor decompositions. Examples include methods like optimized virtual orbital space<sup>81–84</sup> (OVOS), frozen natural orbitals<sup>48,85–87</sup> (FNO), orbital-specific virtuals<sup>88–91</sup> (OSV), and even some local correlation treatments based on, e.g., local pair natural orbitals<sup>92–96</sup> (LPNO).

## 2 Preliminaries

### 2.1 Coupled cluster theory

In this work we adopt a particular convention regarding the indices appearing in the expressions. A detailed explanation is given in Table 1. The canonical Hartree-Fock determinant, denoted  $|\phi_0\rangle$ , is assumed as the reference wavefunction and the spin-orbital energies are given

Table 1: Details of the notation adopted in the present work;  $O$  is the number of active (correlated) orbitals occupied in the reference,  $V$  is the number of virtual orbitals.

Indices	Meaning	Range
$i, j, k, l, \dots$	active orbitals occupied in the reference	$O$
$a, b, c, d, \dots$	orbitals unoccupied in the reference (virtual)	$V$
$p, q, r, s, \dots$	general orbitals (occupation not specified)	$N$
$\mu, \sigma, \lambda, \nu, \dots$	one-particle (atomic) basis set	$N$
$P, Q, \dots$	density fitting auxiliary basis set	$N_{\text{aux}}$
$X, Y, Z, \dots$	compressed subspace of the triply excited amplitudes	$N_{\text{SVD}}$

by  $\epsilon_p$ . The usual partitioning of the electronic Hamiltonian,  $H = F + W$ , into the sum of the total Fock operator ( $F$ ) and the fluctuation potential ( $W$ ) is used throughout this paper. The singly, doubly, triply, etc., excited state determinants are denoted by  $|i^a\rangle$ ,  $|ij^{ab}\rangle$ ,  $|ijk^{abc}\rangle$ , and so forth. For further use we also introduce the following conventions:  $\langle A \rangle \stackrel{\text{def}}{=} \langle \phi_0 | A \phi_0 \rangle$ ,  $\langle i^a | A \rangle \stackrel{\text{def}}{=} \langle i^a | A \phi_0 \rangle$ , and  $\langle A | B \rangle \stackrel{\text{def}}{=} \langle A \phi_0 | B \phi_0 \rangle$  for arbitrary operators  $A, B$ . All equations reported in this work were derived for closed-shell systems in the spin-restricted formalism.

In the coupled cluster theory the electronic wavefunction is parameterized by an exponential Ansatz

$$|\Psi\rangle = e^T |\phi_0\rangle, \quad (2)$$

where  $T = \sum_{n=1} T_n$  is the cluster operator that depends on the single ( $t_i^a$ ), double ( $t_{ij}^{ab}$ ), triple ( $t_{ijk}^{abc}$ ), etc., excitation amplitudes as defined in Ref. 8. The coupled-cluster equations that are used to determine the amplitudes are obtained by inserting the Ansatz (2) into the electronic Schrödinger equation, multiplying by  $e^{-T}$  from the left, and projecting onto a proper subset of excited state determinants. This gives rise to the coupled-cluster residual tensors

$$R_i^a = \langle i^a | e^{-T} H e^T \rangle, \quad R_{ij}^{ab} = \langle ij^{ab} | e^{-T} H e^T \rangle, \quad \text{etc.} \quad (3)$$

They are exactly zero for converged amplitudes, but must be re-calculated a number of times during the coupled-cluster iterations. In this work we are concerned with the CCSDT theory where the cluster operator is truncated at the level of triples, i.e.,  $T = T_1 + T_2 + T_3$ . The corresponding residual tensors can be written as

$$R_i^a = R_i^a(\text{ccsd}) + \langle_i^a | [W, T_3] \rangle, \quad (4)$$

$$R_{ij}^{ab} = R_{ij}^{ab}(\text{ccsd}) + \langle_{ij}^{ab} | [\tilde{F} + \tilde{W}, T_3] \rangle, \quad (5)$$

where  $R_i^a(\text{ccsd})$  and  $R_{ij}^{ab}(\text{ccsd})$  originate from the CCSD theory and depend only on  $T_1$  and  $T_2$  (explicit expressions can be found, for example, in Refs. 97,98), and

$$\begin{aligned} R_{ijk}^{abc} = & \langle_{ijk}^{abc} | [\tilde{F}, T_3] \rangle + \langle_{ijk}^{abc} | [\tilde{W}, T_2] \rangle + \frac{1}{2} \langle_{ijk}^{abc} | [[\tilde{F} + \tilde{W}, T_2], T_2] \rangle \\ & + \langle_{ijk}^{abc} | [\tilde{W}, T_3] \rangle + \langle_{ijk}^{abc} | [[W, T_2], T_3] \rangle. \end{aligned} \quad (6)$$

Throughout the present work we employ the  $T_1$ -similarity-transformed formalism based on the operators  $\tilde{F} = e^{-T_1} F e^{T_1}$  and  $\tilde{W} = e^{-T_1} W e^{T_1}$ . Correspondingly, the ‘‘dressed’’ two-electron integrals, defined precisely in Ref. 97, are denoted by  $(pq|\tilde{r}s)$ . The main advantage of this formalism is that the singly-excited amplitudes can be absorbed into the two-electron integrals, thereby reducing the length of the working equations significantly. While this comes at a price of performing four-index integral transformation during every coupled-cluster iteration, the cost of this procedure is marginal when the density fitting approximation is in effect. Explicit expressions for the CCSDT residuals given in terms of basic one- and two-electron integrals, and the cluster amplitudes are known in the literature.<sup>24</sup> For closed-shell systems one obtains in the present notation

$$R_i^a = R_i^a(\text{ccsd}) + [2(jb|kc) - (jc|kb)] (t_{ijk}^{abc} - t_{ijk}^{bac}), \quad (7)$$



and

$$\begin{aligned}
R_{ij}^{ab} = & R_{ij}^{ab}(\text{ccsd}) + P_2 \left[ \tilde{F}_{kc} (t_{ijk}^{abc} - t_{ijk}^{acb}) \right. \\
& + (ac|\tilde{k}d) (2t_{ijk}^{cbd} - t_{ijk}^{cdb} - t_{ijk}^{dbc}) \\
& \left. - (ki|\tilde{l}c) (2t_{ljk}^{cba} - t_{ljk}^{bca} - t_{ljk}^{abc}) \right], \tag{8}
\end{aligned}$$

where  $P_2 = \binom{ab}{ij} + \binom{ba}{ji}$ . Moving to the triples residual let us first define ‘‘long’’ and ‘‘short’’ permutation operators as

$$\mathcal{P}_L = \binom{abc}{ijk} + \binom{acb}{ikj} + \binom{bac}{jik} + \binom{cab}{kij} + \binom{bca}{jki} + \binom{cba}{kji}, \tag{9}$$

$$\mathcal{P}_S = \binom{abc}{ijk} + \binom{bac}{jik} + \binom{cba}{kji}, \tag{10}$$

respectively, where the notation for the orbital index permutations is the same as in Ref. 100, for example,  $\binom{acb}{ikj}$  permutes the compound indices  $bj$  and  $ck$ , while  $\binom{bca}{jki}$  permutes  $bj$  and  $ck$ , and then  $ai$  and  $bj$ . This allows us to write

$$\begin{aligned}
R_{ijk}^{abc} = & \mathcal{P}_L \left[ t_{il}^{ab} \Xi_{ck}^{lj} - t_{ij}^{ad} \Xi_{ck}^{bd} \right] + \mathcal{P}_S \left[ \chi_{li} t_{ljk}^{abc} - \chi_{ad} t_{ijk}^{dbc} - \chi_{lj}^{mk} t_{ilm}^{abc} - \chi_{bd}^{ce} t_{ijk}^{ade} \right. \\
& \left. + \chi_{ad}^{li} t_{ljk}^{dbc} + \chi_{bd}^{li} t_{ljk}^{adc} + \chi_{cd}^{li} t_{ljk}^{abd} - \chi_{ai}^{ld} (2t_{ljk}^{dbc} - t_{ljk}^{cbd} - t_{ljk}^{bdc}) \right], \tag{11}
\end{aligned}$$

where a handful of intermediates have been introduced

$$\chi_{li} = \tilde{F}_{li} + (me|ld) \bar{t}_{im}^{de}, \quad \chi_{ad} = \tilde{F}_{ad} - (me|ld) \bar{t}_{im}^{ae}, \tag{12}$$

$$\chi_{lj}^{mk} = (lj|\tilde{m}k) + (ld|me) t_{jk}^{de}, \quad \chi_{bd}^{ce} = (bd|\tilde{c}e) + (ld|me) t_{lm}^{bc}, \tag{13}$$

$$\chi_{ad}^{li} = (ad|\tilde{l}i) - (le|md) t_{mi}^{ae}, \quad \chi_{ai}^{ld} = (ai|\tilde{l}d) - (le|md) t_{im}^{ae} + (ld|me) \bar{t}_{im}^{ae}, \tag{14}$$

where the symbol  $\bar{t}_{ij}^{ab}$  is a shorthand notation for  $\bar{t}_{ij}^{ab} = 2t_{ij}^{ab} - t_{ij}^{ba}$ , and

$$\begin{aligned} \Xi_{ck}^{lj} = & (ck|\tilde{l}j) + (lj|\tilde{m}d) \bar{t}_{mk}^{dc} - (ld|\tilde{m}j) t_{mk}^{dc} - (ld|\tilde{m}k) t_{mj}^{cd} \\ & + (cd|\tilde{l}e) t_{kj}^{de} + (ld|me) (2t_{mkj}^{ecd} - t_{mkj}^{ced} - t_{mkj}^{dce}), \end{aligned} \quad (15)$$

$$\begin{aligned} \Xi_{ck}^{bd} = & (ck|\tilde{b}d) - \tilde{F}_{ld} t_{lk}^{bc} + (lk|\tilde{m}d) t_{lm}^{cb} + (bd|\tilde{l}e) \bar{t}_{lk}^{ec} - (be|\tilde{l}d) t_{lk}^{ec} \\ & - (ld|\tilde{c}e) t_{lk}^{be} - (ld|me) (2t_{mkl}^{ecb} - t_{mkl}^{ceb} - t_{mkl}^{bce}). \end{aligned} \quad (16)$$

Let us analyse the computational costs of evaluating the CCSDT residual tensor. The  $R_i^a$  and  $R_{ij}^{ab}$  residuals scale as  $O^3V^3$  and  $O^3V^4$  in the leading-order and thus they do not constitute a bottleneck in the ordinary CCSDT calculations. Concerning the triples residual, computation of all intermediates denoted by the letter  $\chi$  scales as  $N^6$  (or less) with the size of the system. The most expensive among these intermediates is  $\chi_{bd}^{ce}$  and its computational costs ( $O^2V^4$ ) are very similar to the so-called ‘‘particle-particle ladder diagram’’ from the CCSD theory. The  $\Xi_{ck}^{lj}$  and  $\Xi_{ck}^{bd}$  intermediates are more expensive with the leading-order terms scaling as  $O^4V^3$  and  $O^3V^4$ , respectively, due to presence of triply excited amplitudes tensor in the last term of Eq. (15) and Eq. (16). However, the most problematic terms are present in the triples residual tensor, Eq. (11). The terms in the first square bracket and the first two terms in the second square bracket scale as  $N^7$  while all of the remaining ones as  $N^8$ . The most expensive amongst the latter is the diagram involving five virtual indices,  $\chi_{bd}^{ce} t_{ijk}^{ade}$ , which thus scales as  $O^3V^5$  and is typically the bottleneck in CCSDT calculations for larger systems. An important conclusion of this analysis is that if the cost of the CCSDT method is to be reduced to the level of  $N^6$ , all  $\chi$  intermediates, defined by Eqs. (12)-(14), may be calculated as they stand but the scaling of all remaining terms in Eq. (11) must be reduced. Let us also note that in the conventional CCSDT calculations there is no way to avoid storing the triples residual tensor ( $R_{ijk}^{abc}$ ) in core memory which incurs roughly  $\frac{1}{6}O^3V^3$  memory cost.

## 2.2 Decomposition of the integrals

To decompose the electron repulsion integrals tensor,  $(pq|rs)$ , the following symmetric formula is used in this work

$$(pq|rs) = B_{pq}^Q B_{rs}^Q, \quad (17)$$

where  $Q$  is some auxiliary basis set (ABS). Analogous notation is employed for the “dressed” two-electron integrals, i.e.,  $(pq|\tilde{r}s) = \tilde{B}_{pq}^Q \tilde{B}_{rs}^Q$ . Note that  $(ia|\tilde{j}b) = (ia|jb)$  and thus  $\tilde{B}_{ia}^Q = B_{ia}^Q$ .

The generic formula (17) encompasses two the most popular approximations – the density fitting and the Cholesky decomposition. These two techniques differ only in the way of selecting the expansion basis,  $Q$ . In DF method this basis is carefully pre-optimized for each atom and orbital basis set combination. Since ABS functions obtained in this way are not orthogonal, the expansion coefficients are calculated as

$$B_{pq}^Q = (pq|P) [\mathbf{V}^{-1/2}]_{PQ}, \quad (18)$$

where  $(pq|P)$  and  $V_{PQ} = (P|Q)$  are the three-centre and two-centre electron repulsion integrals, respectively (see Ref. 99 for more precise definitions). By contrast, in the CD approach the auxiliary basis is composed of pairs of functions from the original (orbital) basis set. Therefore, this technique requires no additional external input; moreover, it is easier to control the accuracy. In our DF-CC implementation the “dressed” integrals are formed directly from the DF representation of the two-electron integrals in the AO basis during every coupled-cluster iteration.

From the point of view of the present work it is critical to note that both in DF and CD approximations the size of the ABS ( $N_{\text{aux}}$ ) scales linearly with the size of the system. This is obvious in case of the DF technique where the ABS for a molecule is simply a union of auxiliary basis sets of the constituting atoms. One can thus write  $N_{\text{aux}} = c_{\text{aux}} N$  and, in

practice, we have  $c_{\text{aux}} \in 2-5$ . In the CD approach the asymptotic linear scaling of  $N_{\text{aux}}$  was demonstrated numerically,<sup>52</sup> but somewhat larger values of  $c_{\text{aux}}$  may be needed to reach the accuracy levels characteristic for DF.<sup>47,48</sup>

Let us stress that the application of the decomposition (17) alone does not improve the overall scaling of the CCSDT method. As an example consider the term  $\chi_{bd}^{ce} t_{ijk}^{ade}$ . The intermediate  $\chi_{bd}^{ce}$  does not factorize naturally to the form analogous to Eq. (17) because of the second term in Eq. (13). Moreover, even if such factorization was forced, e.g., by performing the Cholesky decomposition  $\chi_{bd}^{ce} = L_{bd}^Q L_{ce}^Q$  during every iteration, the resulting working expression,  $L_{bd}^Q (L_{ce}^Q t_{ijk}^{ade})$ , would still require  $N^8$  computational effort to evaluate.

### 2.3 Decomposition of the $T_3$ amplitudes

The most troublesome issue related to the Tucker-3 compression format, Eq. (1), is the necessity to compute the basic expansion tensors,  $U_{ai}^X$ . For convenience of the readers we briefly summarize the optimal strategy to find these quantities. Assume that are given some approximate triples amplitude tensor. In the present work we employ the following formula

$${}^{(2)}t_{ijk}^{abc} = (\epsilon_{ijk}^{abc})^{-1} \langle abc |_{ijk} [\widetilde{W}, T_2] \rangle, \quad (19)$$

where the  $T_1$  and  $T_2$  amplitudes are taken from the CCSD theory. The superscript “(2)” was added to distinguish Eq. (19) from the exact CCSDT amplitudes tensor and signifies that this formula is accurate only through the second order in perturbation theory. Eq. (19) is obtained by retaining only the first two terms of Eq. (6), similarly as in the CC3 model. Compared to our previous work<sup>36</sup> the “dressed” fluctuation potential  $\widetilde{W}$  is used in Eq. (19) instead of  $W$ . This is due to a unique role of single excitations as approximate orbital relaxation parameters which may help to improve the results in quasi-degenerate situations. Other than that, the results obtained with  $W$  and  $\widetilde{W}$  should be very close, as are their computational costs. Let us stress that the choice given by Eq. (19), although natural and

self-contained, is arbitrary and the method presented in this work is applicable also for other sources of approximate triple amplitudes.

Having the approximate tensor  ${}^{(2)}t_{ijk}^{abc}$  we perform its “flattening”, i.e., rewrite it as a rectangular matrix with dimensions  $O^2V^2 \times OV$ , giving  ${}^{(2)}t_{aibj,ck}$ . Next, the singular-value decomposition of this matrix is performed. The left singular vectors are discarded while the right singular vectors constitute the desired basis,  $U_{ai}^X$ . To obtain the optimal compression of the full tensor  $t_{ijk}^{abc}$  to a desired size  $N_{\text{SVD}}$ , one retains only those vectors  $U_{ai}^X$  that correspond to the largest singular values of the “flattened” matrix (note that the singular values are non-negative real numbers). Unfortunately, if a complete singular value decomposition of the  ${}^{(2)}t_{aibj,ck}$  were to be performed (and subsequently the insignificant singular values/vectors were simply dropped), the computational cost of the procedure would scale as  $N^8$ . To avoid this we have recently introduced a technique based on Golub-Kahan bidiagonalization<sup>101</sup> which enables to selectively find a predefined number of singular vectors of the matrix  ${}^{(2)}t_{aibj,ck}$  that correspond to the *largest* singular values. Since in practice only a small number of singular vectors (compared with the dimension of the full  $t_{ijk}^{abc}$  tensor) is needed in Eq. (1) to obtain a decent accuracy, significant time savings are achieved. The method is composed mostly of left/right multiplications of the matrix  ${}^{(2)}t_{aibj,ck}$  by some trial vectors, and thus its formal scaling is proportional to  $N_{\text{SVD}} O^3V^3 \propto N^7$ . However, in comparison with the previous work we managed to exploit the fact that the sparsity of the  ${}^{(2)}t_{aibj,ck}$  tensor also increases with the system size. A combination of screening techniques with sparse matrix-vector multiplication routines have enabled us to reduce the computational effort of the procedure considerably. In practical applications we observed numerically that the effective scaling of the method is usually in-between  $N^6$  and  $N^7$  for larger molecules, as demonstrated further in the paper, despite the more pessimistic theoretical estimate. Nevertheless, the formal scaling of this step is  $N^7$  in the worst-case scenario.

The success of the Tucker-3 compression format, Eq. (1), is based on the fact that the dimension of the compressed tensor  $t_{XYZ}$  can be made significantly smaller than the of the  $t_{ijk}^{abc}$

tensor ( $OV$ ) without sacrificing much of accuracy. To quantify the rate of the compression on a relative basis let us define the *compression factor* as  $\rho = N_{\text{SVD}}/OV$ . Clearly, one has  $\rho \leq 1$  and the results become exact when  $\rho \rightarrow 1$ . One of the most important aspects of Eq. (1) is the scaling of  $N_{\text{SVD}}$  with the system size. Let us first consider the case when both  $O$  and  $V$  are simultaneously increased. To maintain a constant relative accuracy in the correlation energy the value of  $N_{\text{SVD}}$  must increase only linearly with the system size, i.e.,  $N_{\text{SVD}} \propto N$ . This has been demonstrated recently at the CC3<sup>100</sup> level of theory for chains of beryllium atoms with increasing length,<sup>36</sup> and in the present work we provide further numerical evidence by considering a more chemically appealing example of linear alkanes. It is also worth mentioning that virtually the same conclusion regarding the dimension of the compressed tensor has recently been reported by Parrish et al.<sup>39</sup> at the CCSD level of theory. They have considered a compression of  $t_{ij}^{ab}$  in the form  $t_{ij}^{ab} = t_{XY} U_{ai}^X U_{bj}^Y$ , where  $U_{ai}^X$  are the eigenvectors of MP2 or MP3 amplitudes corresponding to the eigenvalues of the largest magnitude, and proven that to maintain a constant relative accuracy in the correlation energy, the dimension of the tensor  $t_{XY}$  must scale only linearly with the system size. Therefore, this appears to be a more general conclusion that may be equally valid for analogues of Eq. (1) in higher dimensions. Additionally, we must stress that while the quantity  $\rho$  is useful in illustrating the compression rate obtained for a given system (for example, with different basis sets) it is not transferable between molecules of different size. In fact, because  $N_{\text{SVD}}$  scales linearly with the system size,  $\rho$  decreases and eventually vanishes as the system size grows.

It is also important to discuss the scaling of  $N_{\text{SVD}}$  in a different case – the value of  $O$  is fixed and only  $V$  is increased. This corresponds to a situation where, e.g., one performs calculations for the same system increasing only the basis set size. It has been shown<sup>36</sup> that in such case the optimal value of  $\rho$  that maintains a constant relative accuracy decreases, albeit rather slowly. For example, for a set of a dozen or so small molecules considered in Ref. 36 the average optimal  $\rho$  was found to be 12.5% for cc-pVDZ basis set and decreased to 9.2% for cc-pVQZ. Therefore,  $N_{\text{SVD}}$  scales sub-linearly with  $V$  but the exact scaling is

difficult to quantify and may depend on the basis set family, presence of linear dependencies, and numerous other factors.

## 3 Theory

### 3.1 Overview

In this section we present detailed working equations of an approximate CCSDT method where single and double excitations are treated in a conventional way while the compression given by Eq. (1) is employed for the triply excited amplitudes. For brevity we shall refer to this method as SVD-CCSDT in the remainder of the text.

In methods that employ rank-reduction techniques to reduce its computational burden it is critical that the calculations are performed without “unpacking” the compressed quantities to its original dimension at any stage. Therefore, in the SVD-CCSDT method the  $t_{ijk}^{abc}$  tensor never appears explicitly and is replaced by its compressed counterpart,  $t_{XYZ}$ . Similarly, instead of evaluating the triples residual  $R_{ijk}^{abc}$ , only the following compressed quantity

$$r_{XYZ} = U_{ai}^X U_{bj}^Y U_{ck}^Z R_{ijk}^{abc}, \quad (20)$$

is exploited in the calculations. Note that  $r_{XYZ}$  is fully symmetric with respect to exchange of all its indices. As a byproduct of the SVD procedure the tensors  $U_{ai}^X$  form an orthonormal basis

$$U_{ai}^X U_{ai}^Y = \delta_{XY}. \quad (21)$$

While not strictly necessary it is also beneficial to follow Ref. 33 and enforce the relationship

$$U_{ai}^X U_{ai}^Y (\epsilon_i - \epsilon_a) = \epsilon_X \delta_{XY}, \quad (22)$$

where  $\epsilon_X$  are real-valued constants, which is achieved by a unitary rotation among the original  $U_{ai}^X$  tensors. This leads to a simple prescription for an update of the compressed triple excitation amplitudes

$$\frac{r_{XYZ}}{\epsilon_X + \epsilon_Y + \epsilon_Z} \rightarrow t_{XYZ}. \quad (23)$$

In other words, during every coupled cluster iteration the residual tensor  $r_{XYZ}$  divided by the denominator  $\epsilon_X + \epsilon_Y + \epsilon_Z$  is added to the “old” compressed triples tensor. This obviously leads to convergence when the CC iterations are solved, i.e. when  $r_{XYZ} = 0$ .

An extensive justification of an analogous scheme at the CCSD level of theory has been given in the work of Parrish et al.<sup>39</sup> where a Lagrangian form of the coupled-cluster equations is used to define a suitable stationary condition allowing for optimization of the amplitudes. This formalism is straightforward to generalize to the present case if the triply de-excited component of the  $\Lambda$ -amplitudes is written in a form analogous to Eq. (1). Let us also point out that due to relatively small size of the compressed triple amplitudes tensor ( $N^3$  scaling) several instances of it can be stored simultaneously. This allows to exploit techniques such as direct inversion of iterative subspace (DIIS),<sup>102,103</sup> or similar methods<sup>104–106</sup> that accelerate the convergence of the coupled-cluster equations, with  $r_{XYZ}$  being a natural candidate for the error vector.

### 3.2 Evaluation of the $R_i^a$ and $R_{ij}^{ab}$ residuals

In this section we consider triples contribution to the singles and doubles residuals given by Eqs. (7) and (8). In the evaluation of these contributions it is convenient to exploit the



following intermediates

$$B_{ia}^{QX} = \tilde{B}_{ji}^Q U_{aj}^X, \quad (24)$$

$$B_{ai}^{QX} = \tilde{B}_{ab}^Q U_{bi}^X, \quad (25)$$

$$B_{ij}^{QX} = B_{ia}^Q U_{aj}^X, \quad (26)$$

$$A_X^Q = B_{ia}^Q U_{ai}^X. \quad (27)$$

The storage requirements for the first three intermediates scale as  $N^4$ , but it is not necessary to read them into memory in full at any stage of the computations. These definitions allow us to rewrite the triples contribution to the singles residual as

$$\begin{aligned} \langle_i^a | [W, T_3] \rangle &= U_{ai}^X \left[ t_{XYZ} \left( 2A_Y^Q A_Z^Q - B_{jk}^{QZ} B_{kj}^{QY} \right) \right] \\ &\quad - U_{aj}^Y \left[ 2B_{ji}^{QX} \left( t_{XYZ} A_Z^Q \right) - t_{XYZ} \left( B_{jk}^{QZ} B_{ki}^{QX} \right) \right]. \end{aligned} \quad (28)$$

The last term in the above expression is the most expensive, scaling as  $O^3 N_{\text{aux}} N_{\text{SVD}}^2 \propto N^6$ . Note that the presence of some of the brackets in the above equation are not necessary from the mathematical point of view; they are introduced to underline the order of operations that leads to the optimal scaling of the computational costs for the respective terms. The same convention is adopted in the remainder of the text.

For the doubles residual one obtains an analogous factorization

$$\begin{aligned} \langle_{ij}^{ab} | [\tilde{F} + \tilde{W}, T_3] \rangle &= P_2 \left[ U_{ai}^X U_{bj}^Y \left( t_{XYZ} (\tilde{F}_{kc} U_{ck}^Z) \right) - U_{ai}^X \left( t_{XYZ} U_{bk}^Z \right) (\tilde{F}_{kc} U_{cj}^Y) \right. \\ &\quad + 2 U_{bj}^Y \left( (B_{ia}^{QZ} - B_{ai}^{QZ}) (A_X^Q t_{XYZ}) \right) - (B_{ia}^{QZ} - B_{ai}^{QZ}) \left( \underline{B_{kj}^{QY} (U_{bk}^X t_{XYZ})} \right) \\ &\quad \left. - (U_{bj}^Z t_{XYZ}) \left( \underline{B_{ak}^{QX} B_{ki}^{QY}} - U_{ak}^Y (B_{ic}^{QX} B_{kc}^Q) \right) \right]. \end{aligned} \quad (29)$$

The computational costs of evaluating all terms in the above expression scale as  $N^5$  (or less) except for the two underlined terms which scale as  $N^6$  or, more precisely, as  $N_{\text{SVD}}^2 O^2 V N_{\text{aux}}$  in the rate-determining step. In order to roughly compare this with the scaling of the

uncompressed doubles residual ( $O^3V^4$  in the leading-order term) we set  $N_{\text{SVD}} \approx V$ . In practical applications the ratio  $N_{\text{SVD}}/V$  is only somewhat larger than the unity with double-zeta basis sets, and somewhat smaller than the unity with triple-zeta (or better) basis sets. The speed-up in the evaluation of the doubles residual is thus proportional to  $\frac{N_{\text{aux}}}{OV}$ . Finally, the size of the auxiliary basis set is typically several times larger than  $V$  and the ratio of 2–5 is a reasonable estimate. Therefore, a considerable speed-up in evaluation of the doubles residual tensor according to Eq. (29) is expected only when  $O$  is large and this has been observed in calculations reported in the next section of this work.

### 3.3 Evaluation of the compressed triples residual

While the ability to calculate the doubles residual at a reduced cost for large systems is certainly advantageous, this step does not constitute the bottleneck in the full CCSDT calculations. The true proving ground for the decomposition strategy adopted in this work is the evaluation of the compressed triples residual, Eq. (20). In this section we present fully factorized equations that prove that computation of  $r_{XYZ}$  can be accomplished with  $N^6$  cost. To this end, we first define permutation operators analogous to Eqs. (9) and (10) but acting on the indices of the SVD basis

$$\mathcal{P}'_L = (XYZ) + (XZY) + (YXZ) + (ZXY) + (YZX) + (ZYX), \quad (30)$$

$$\mathcal{P}'_S = (XYZ) + (YXZ) + (ZYX), \quad (31)$$

and note that for an arbitrary tensor  $A_{ijk}^{abc}$  one has

$$U_{ai}^X U_{bj}^Y U_{ck}^Z \left( \mathcal{P}'_L A_{ijk}^{abc} \right) = \mathcal{P}'_L \left( U_{ai}^X U_{bj}^Y U_{ck}^Z A_{ijk}^{abc} \right), \quad (32)$$

and similarly for the “short” permutation.

Let us define half-transformed doubles amplitudes as

$$T_{ai}^X = U_{bj}^X t_{ij}^{ab}, \quad S_{ai}^X = U_{bj}^X t_{ij}^{ba}, \quad \bar{T}_{ai}^X = 2T_{ai}^X - S_{ai}^X \quad (33)$$

along with a new class of intermediates

$$\begin{aligned} \chi_{XY}^{\text{occ}} &= U_{al}^X (\chi_{li} U_{ai}^Y), & \chi_{XY}^{\text{vir}} &= U_{ai}^X (\chi_{ad} U_{di}^Y), \\ \chi_{XY}^{\text{mix}} &= U_{ai}^X (\chi_{ad}^{li} U_{dl}^Y), & \chi_{ld}^X &= \chi_{ai}^{ld} U_{ai}^X, \end{aligned} \quad (34)$$

$$\chi_{mk}^{XY} = U_{bj}^X (\chi_{lj}^{mk} U_{bl}^Y), \quad \chi_{ce}^{XY} = U_{bj}^X (\chi_{bd}^{ce} U_{dj}^Y), \quad \Pi_{li}^{XY} = U_{bj}^X (\chi_{bd}^{li} U_{dj}^Y), \quad (35)$$

and

$$\Xi_{lj}^Z = \Xi_{ck}^{lj} U_{ck}^Z, \quad \Xi_{bd}^Z = \Xi_{ck}^{bd} U_{ck}^Z. \quad (36)$$

As discussed above, calculation of all  $\chi$  intermediates given by Eqs. (12)-(14) scales as  $N^6$  or less. Similarly, in Eqs. (34)-(35) none of the the step-wise contractions involve more than six indices at the same time and thus can be calculated with the computational effort of at most  $N^6$ . A more challenging problem is the evaluation of the last two intermediates, see Eq. (36), because calculation of  $\Xi_{ck}^{lj}$  and  $\Xi_{ck}^{bd}$  themselves requires an  $N^7$  step. Fortunately, by combining Eqs. (15) and (16) with the integral decomposition (17), and by manipulating the order of multiplications one can show that the intermediate  $\Xi_{bd}^Z$  can equivalently be rewritten as

$$\begin{aligned} \Xi_{bd}^Z &= \tilde{B}_{bd}^Q (\tilde{B}_{ck}^Q U_{ck}^Z) - \tilde{F}_{ld} T_{bl}^Z + \underline{U_{ck}^Z (t_{lm}^{cb} (\tilde{B}_{lk}^Q B_{md}^Q))} + \tilde{B}_{bd}^Q (B_{le}^Q \bar{T}_{el}^Z) \\ &\quad - B_{ld}^Q (\tilde{B}_{be}^Q T_{el}^Z) - B_{ld}^Q (t_{lk}^{be} (U_{ck}^Z \tilde{B}_{ce}^Q)) - \underline{2B_{ld}^Q (U_{bl}^{Z'} (t_{X'ZZ'} A_{X'}^Q))} \\ &\quad + \underline{B_{ld}^Q (U_{bl}^{Z'} (B_{me}^Q (U_{ek}^{Y'} (t_{X'Y'Z'} (U_{cm}^{X'} U_{ck}^Z)))))} + t_{X'Y'Z} (U_{bm}^{Y'} (B_{ld}^Q \tilde{B}_{ml}^{QX'})). \end{aligned} \quad (37)$$

Calculation of all terms in the above expression scales as  $N^5$  or less except for the three underlined terms that contain  $N^6$  (outer) leading-order steps scaling as  $O^3V^3$ ,  $O^2V^2N_{\text{SVD}}N_{\text{aux}}$ , and  $O^2N_{\text{SVD}}^4$ , in the order of appearance. There are no terms scaling as  $N^7$  or higher. Similarly for the  $\Xi_{ij}^Z$  intermediate one obtains

$$\begin{aligned}
\Xi_{ij}^Z &= \tilde{B}_{ij}^Q (\tilde{B}_{ck}^Q U_{ck}^Z) + \tilde{B}_{ij}^Q (B_{md}^Q \bar{T}_{dm}^Z) - \tilde{B}_{mj}^Q (B_{ld}^Q T_{dm}^Z) - U_{ck}^Z \left( t_{mj}^{cd} (B_{ld}^Q \tilde{B}_{mk}^Q) \right) \\
&+ U_{ck}^Z \left( t_{kj}^{de} (B_{le}^Q \tilde{B}_{cd}^Q) \right) + 2B_{ld}^Q \left( U_{dj}^{Z'} (t_{X'ZZ'} A_{X'}^Q) \right) \\
&- B_{ld}^Q \left( U_{dj}^{Z'} \left( B_{me}^Q (U_{ek}^{Y'} (t_{X'Y'Z'} (U_{cm}^{X'} U_{ck}^Z))) \right) \right) + t_{X'ZZ'} (B_{lm}^{QX'} B_{mj}^{QZ'}).
\end{aligned} \tag{38}$$

One may notice that many terms present in Eq. (38) bare close resemblance to analogous terms in Eq. (37). Indeed, in a careful implementation many intermediate quantities necessary for evaluation of  $\Xi_{bd}^Z$  can be reused when  $\Xi_{ij}^Z$  is constructed simultaneously. This allows to compute  $\Xi_{ij}^Z$  essentially as a byproduct with only a handful of additional terms that need to be evaluated separately. The latter terms are relatively inexpensive since they scale as  $O^3N_{\text{SVD}}^2N_{\text{aux}}$  or similarly.

Finally, we pass to the calculation of the compressed triples residual tensor, Eq. (20).

With help of the intermediates defined above it can be rewritten as

$$\begin{aligned}
r_{XYZ} &= \mathcal{P}'_L \left[ \left( T_{bl}^X \Xi_{ij}^Z - \Xi_{bd}^Z T_{dj}^X \right) U_{bj}^Y \right] + \mathcal{P}'_S \left[ \chi_{X'X}^{\text{occ}} t_{X'YZ} - \chi_{X'X'}^{\text{vir}} t_{X'YZ} \right. \\
&+ \chi_{X'X'}^{\text{mix}} \left( t_{X'Y'Z} (U_{bj}^Y U_{bj}^{Y'}) \right) - 2t_{X'YZ} (\chi_{ld}^X U_{dl}^{X'}) \\
&- U_{ck}^Z \left( \chi_{mk}^{YY'} (t_{XY'Z'} U_{cm}^{Z'}) \right) - \underline{U_{ck}^Z \left( \chi_{ce}^{YY'} (t_{XY'Z'} U_{ek}^{Z'}) \right)} \\
&+ U_{ai}^X \left( U_{al}^{X'} (t_{X'Y'Z} \Pi_{li}^{YY'} + t_{X'YZ'} \Pi_{li}^{ZZ'}) \right) \\
&\left. + U_{ck}^Z \left( (t_{X'Y'Y} U_{cl}^{X'}) (\chi_{ld}^X U_{dk}^{Y'}) \right) + U_{bj}^Y \left( (t_{X'Y'Z} U_{bl}^{X'}) (\chi_{ld}^X U_{dj}^{Y'}) \right) \right].
\end{aligned} \tag{39}$$

Computation of the terms in the first square brackets scales as  $N^5$  – less expensive than of the  $\Xi_{ij}^Z$  and  $\Xi_{bd}^Z$  intermediates themselves. The first four terms in the second square brackets scale as  $N^4$ , and thus are not a cause for a major concern, while the remaining

terms in Eq. (39) scale as  $N^6$ . The most expensive part of Eq. (39) is the sixth term in the second square brackets (underlined, scaling as  $OV^2N_{\text{SVD}}^3$ ) resulting from factorization of the  $\chi_{bd}^{ce} \underline{t_{ijk}^{ade}}$  term of the uncompressed triples residual, cf. Eq. (11). This is the only term in the conventional CCSDT method that involves five virtual indices simultaneously, leading to a rate-determining computational step that scales as  $O^3V^5$ . Under the assumption that  $V \approx N_{\text{SVD}}$  we can therefore conclude that the compression method employed in this work reduces the cost of evaluating the CCSDT triples residual by a factor proportional to  $O^2$ .

In the above discussion we have neglected an important issue. The major difference between the conventional CC and SVD-based approaches is the number of consecutive tensor contractions that appear in the working expressions. In the conventional CCSDT residual, Eq. (11), no products containing more than three different tensors are present. Therefore, there are only three possible ways to perform contractions of the constituting tensors and all necessary manipulations can be performed rather easily. In the SVD-based formalism, on the other hand, some quantities contain products of six or seven tensors – see, for example, Eq. (37). The number of ways the tensors can be arranged grows exponentially with the length of the tensor string, and in most cases the order of tensor multiplications effects the final scaling of a given term. Since typically it is not possible to check all reasonable arrangements by hand, most of the derivations presented in this work were accomplished with help of computer algebra<sup>107</sup> which allowed to determine the optimal multiplication order by defining a set of rules.

An additional problem that appears in this context is related to the fact that while the scaling of the computational cost for a given expression is always defined uniquely, the prefactors of two terms with the same scaling are, in general, difficult to compare. For example, the relative cost of two terms with the same scaling may depend on the difference between the ratios  $N_{\text{SVD}}/V$  and  $V/O$ . This difference may change significantly depending on the number of electrons in the system, cardinality of the basis set, desired accuracy threshold, etc. In such problematic cases several variants of a routine handling the same tensor string

should probably be incorporated into the code and the decision which one is to be used should be made on the fly. However, in our pilot implementation reported in this work, we simply selected those factorizations that delivered a reasonable efficiency in a wide range of situations assuming  $O < V \approx N \approx N_{\text{SVD}} < N_{\text{aux}}$  as a rule of thumb.

Finally, let us discuss memory requirements of the SVD-CCSDT method in the present implementation and some technical aspects of handling numerous intermediate quantities that appear in the working equations. The only objects of size  $N^4$  that must be held in core memory are the double excitation amplitudes and the doubles residual tensor (both  $\frac{1}{2}O^2V^2$ ). Other “large” intermediates are either stored on the disk and read in smaller chunks whenever necessary ( $B_{ia}^{QX}$ ,  $B_{ai}^{QX}$ , and  $B_{ij}^{QX}$ ) or are built on-the-fly in a batched loop over one occupied/virtual index ( $\chi_{mk}^{XY}$ ,  $\chi_{ce}^{XY}$ ,  $\Pi_i^{XY}$ ) and contracted immediately. Therefore, there is no need to keep any of them in full in core memory. The remaining quantities require only  $N^3$  memory to store – the largest being either  $\Xi_{bd}^Z$  or  $t_{XYZ}$  depending on the circumstances. To sum up, while the overall memory requirements of the SVD-CCSDT method are significantly larger than of CCSD, the SVD-CCSDT algorithm introduces no large intermediate quantities that would create a serious memory bottleneck. In particular, the uncompressed  $t_{ijk}^{abc}$  and  $R_{ijk}^{abc}$  tensors do not appear at any stage of the calculations which removes the  $N^6$  memory requirement of the conventional CCSDT theory.

## 4 Numerical results and discussion

### 4.1 Computational details

All calculations reported in this work employ Dunning-type cc-pVDZ and cc-pVTZ basis sets.<sup>108</sup> The corresponding auxiliary basis sets (MP2FIT) for the density fitting approximation were taken from the work of Weigend et al.<sup>46,109</sup> Pure spherical representation of both basis sets was used throughout.

The theoretical methods described in the previous sections were implemented in a locally

modified version of the GAMESS program package.<sup>110</sup> The code for the DF decomposition is based on the resolution-of-identity MP2 (RI-MP2) implementation by Katouda and Nagase<sup>99</sup> that is available in the official release of the GAMESS program. DF was used by default at every stage of correlated calculations, i.e., in the remainder of the text the acronyms CCSD, CC3, etc., should be interpreted as DF-CCSD, DF-CC3, and so forth, unless explicitly stated otherwise. The only method where DF is never used is the uncompressed (exact) CCSDT since, to the best of our knowledge, no such implementation is publicly available. Hartree-Fock equations were always solved utilising the exact two-electron integrals. Frozen-core approximation was invoked throughout:  $1s$  orbitals of all first-row atoms were left uncorrelated (inactive) unless explicitly stated otherwise. Geometries of the molecules were optimized at MP2/cc-pVTZ level of theory. The only exceptions are linear alkanes,  $C_nH_{2n+2}$  with  $n = 1, 8$ , which were optimized by using B3LYP/cc-pVTZ method.<sup>111–113</sup> Geometries of all molecules considered in this work can be found in Supporting Information. Other parameters controlling the coupled-cluster calculations and decomposition steps were the same as in Ref. 36.

## 4.2 Scaling with the system size

Before discussing the accuracy of the SVD-CCSDT method we would like to demonstrate that, in calculations for realistic systems, its scaling is consistent with the theoretical findings from the previous section. To this end we performed CC3 and SVD-CC3 calculations for linear alkanes,  $C_nH_{2n+2}$ , with the chain length  $n = 1, \dots, 8$ . For each  $n$  we recorded the optimal size of the SVD subspace,  $N_{\text{SVD}}$ , sufficient to recover 99.9% of the CC3 correlation energy (uncompressed CC3 was used as a benchmark). The results presented in Fig. 1 reveal almost perfect linear relationship between  $N_{\text{SVD}}$  and  $n$  for  $n \geq 2$ . The coefficient of determination for the linear fit to the data with  $n \geq 2$  is higher than 0.999. Next, we performed SVD-CCSDT calculations for the same set of molecules with  $N_{\text{SVD}}$  found at the CC3 level of theory for each  $n$ . Additionally, for  $n = 2 - 6$  we performed the exact

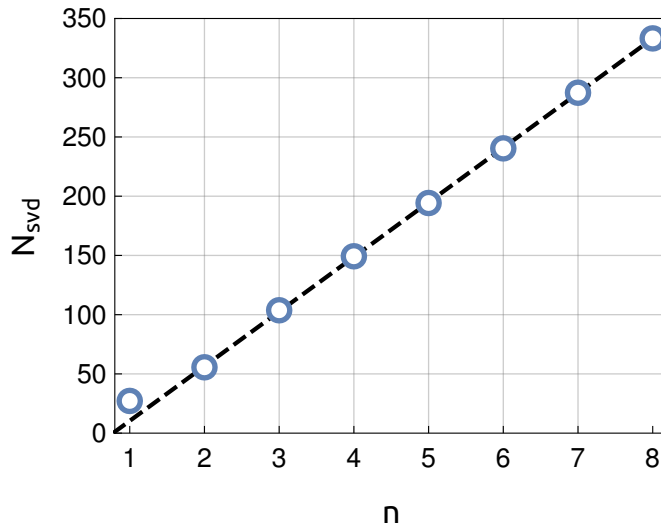


Figure 1: Optimal size of the SVD subspace ( $N_{\text{SVD}}$ ) sufficient to recover 99.9% of the CC3 correlation energy for linear alkanes,  $\text{C}_n\text{H}_{2n+2}$ , as a function of the chain length ( $n$ ).

(uncompressed) CCSDT calculations with the ACESII program package. Unfortunately, for  $n > 6$  a single CCSDT iteration already took more than several days; such calculations would not be feasible in practice and were thus abandoned.

In Fig. 2 we compare timings and scaling of the computational costs separately for

- the exact CCSDT calculations (solid black line);
- SVD-CCSDT calculations with  $N_{\text{SVD}}$  determined at the CC3 level of theory (dashed orange line);
- determination of the SVD expansion tensors,  $U_{ai}^X$  in Eq. (1) (dotted red line),

taking linear alkanes as a benchmark. In each case the time necessary for a single iteration is presented (determination of the SVD subspace is also iterative in nature, see Ref. 36). However, it must be noted that the number of iterations necessary to converge the SVD vectors is usually less than ten, and even five iterations are sufficient for small SVD subspaces. To converge the CCSDT and SVD-CCSDT calculations about 20-30 iterations are usually required (albeit we observed that SVD-CCSDT has a better convergence characteristics than the exact CCSDT in more demanding cases). Therefore, one has to keep in mind that the



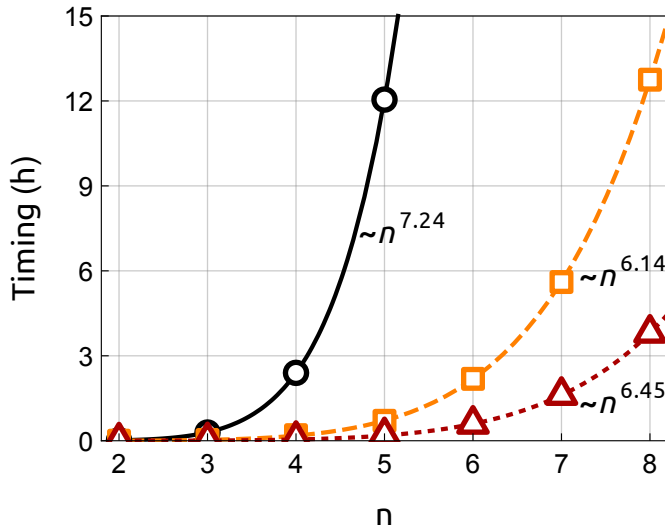


Figure 2: Timings for a single iteration of the CCSDT method (solid black line,  $1.04 \cdot 10^{-4} n^{7.24}$ ), of the SVD-CCSDT method (dashed orange line,  $3.60 \cdot 10^{-5} n^{6.14}$ ) and of the determination of the SVD subspace (dotted red line,  $5.75 \cdot 10^{-6} n^{6.45}$ ) for linear alkanes,  $C_nH_{2n+2}$ , as a function of the chain length ( $n$ ). Power functions obtained by fitting the corresponding data points are given near each graph.

actual total workload required for the determination of the SVD subspace is, under typical circumstances, several times smaller in relation to SVD-CCSDT than the timings for a single iteration would suggest.

The computational timings discussed above were fitted with a power function  $a \cdot n^b$  for  $n \geq 2$ , where  $a$  and  $b$  are adjustable real parameters. Since  $n$  is roughly proportional to number of orbital and auxiliary basis set functions, this allows to “empirically” determine the scaling of the computational costs with the system size. Starting with the CCSDT method, we obtained  $n^{7.24}$  from the fit which is somewhat smaller than the expected  $n^8$ . This can be explained by the fact that the CCSDT calculations were feasible only up to  $n = 6$  which may not be sufficient to reach the asymptotic regime and lower-order terms may still contribute significantly to the total computational time. In the case of the SVD-CCSDT method, where computational timings up to  $n = 8$  were available, the power law fit ( $n^{6.14}$ ) agrees well with the expected scaling of the method. For the determination of the SVD expansion tensors the obtained scaling is  $n^{6.45}$ . This scaling reduction is accompanied by a considerable decrease of the overall computational costs. For example, a single iteration

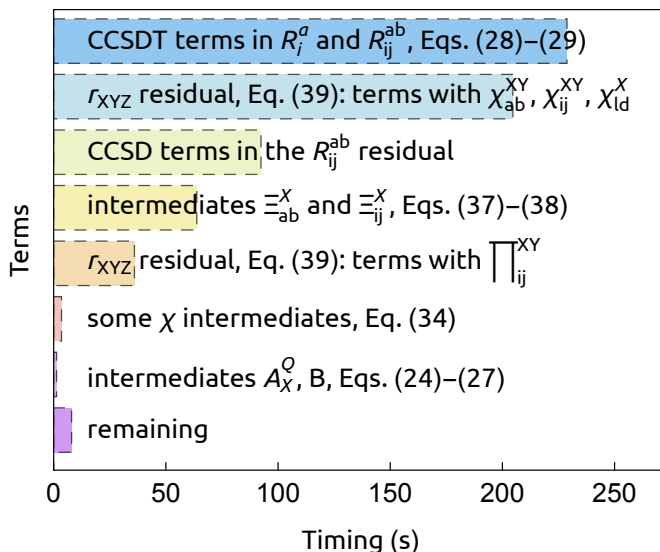


Figure 3: Breakdown of the SVD-CCSDT wall clock timing for the  $\text{HNO}_3$  molecule in the cc-pVTZ basis set ( $O = 12$ ,  $N = 134$ ,  $N_{\text{aux}} = 354$ ,  $N_{\text{SVD}} = 120$ ). All steps that required less than 1 second to complete are accumulated in the “remaining” category. This category also includes the cost of updating the coupled-cluster amplitudes, convergence checks, evaluating the energy, and similar minor tasks performed during every iteration.

of the exact CCSDT method for  $n = 5$  takes a comparable amount of time to a single SVD-CCSDT iteration for  $n = 8$ . By extending the trends shown in Fig. 2 one can also estimate that for  $n = 11 - 12$  the SVD-CCSDT would reach a cost comparable to CCSDT for  $n = 6$ .

It is also interesting to break the computational time spent in a single SVD-CCSDT iteration down into components corresponding to various terms in Eq. (39) and other steps discussed in Sec. 3. For this purpose we selected  $\text{HNO}_3$  molecule in the cc-pVTZ basis set ( $O = 12$ ,  $N = 134$ ,  $N_{\text{aux}} = 354$ ). As shown in the next section, the size of the SVD subspace considered here ( $N_{\text{SVD}} = 120$ ) is sufficient to reach the accuracy of a fraction of kJ/mol in the total correlation energy with respect to the uncompressed result. We thus have  $N_{\text{SVD}} \approx V$  which is a typical phenomenon for the basis sets of this quality. The breakdown of the computational timings is shown in Fig. 3. Rather surprisingly, the most computationally demanding step is evaluation of the triples contribution to the singles and doubles residuals. The next in the order of expense is one of the terms from Eq. (39) that involves the  $\chi_{ab}^{XY}$  intermediate. For comparison, in Fig. 3 we also include the CCSD contribution to the  $R_{ij}^{ab}$

residual which typically consumes more than 90% of the computational time necessary for the conventional CCSD iterations. This allows to compare the cost of various terms present in the SVD-CCSDT theory in relation to the standard CCSD method, revealing that SVD-CCSDT calculations are only 5 – 6 times more expensive than CCSD. Since both methods scale as  $N^6$  with the size of the system, this ratio is likely to remain approximately constant for larger molecules, albeit not necessarily in basis sets that are much larger. Let us point out that all calculations reported here were accomplished by using a single CPU core. However, it has recently been shown that impressive reductions of the CCSDT computational cost are achievable with parallel execution.<sup>114</sup> Since our present SVD-CCSDT implementation consist mostly of lengthy loops over fixed-size batches of occupied, virtual, etc., indices, we believe that a similar efficiency gain is possible, and this option should be considered in future implementations.

### 4.3 Accuracy of the method

To investigate the accuracy of the SVD-CCSDT method in the reproduction of the exact CCSDT energetics we selected four small benchmark molecular systems (methane, ethyne, nitrous oxide, and nitric acid) for which the conventional CCSDT calculations can be performed in a reasonable wall time. We evaluated SVD-CCSDT energies with increasing SVD subspace size (in steps of five at a time) and recorded errors with respect to the exact CCSDT method. Note that in the SVD-CCSDT results there is an additional source of error due to the density fitting approximation. To eliminate this problem from our benchmark calculations we tested two distinct approaches. The first is to use very large auxiliary basis set such as cc-pV6Z-RI (available in the Basis Set Exchange repository<sup>115</sup>). The second idea is to assume that the density-fitting error is the same at the CC3 and CCSDT levels of theory. One can then evaluate the DF-CC3 and conventional CC3 energies separately and correct the SVD-CCSDT results to account for the difference. In all calculations reported here both methods agreed to 0.1 kJ/mol and thus the results reported in this section can be viewed

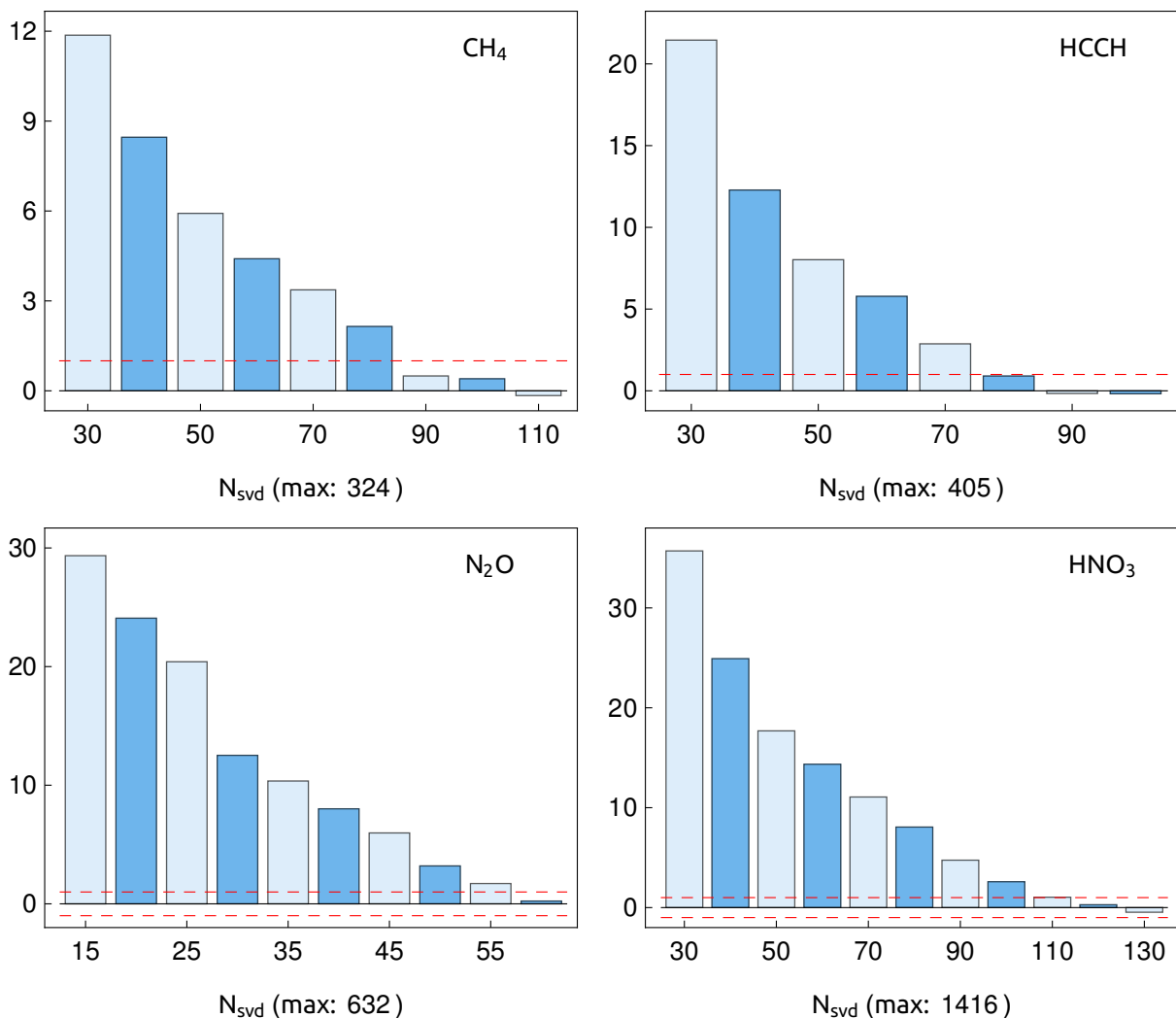


Figure 4: Errors in the SVD-CCSDT correlation energies (in kJ/mol) as a function of the SVD subspace size ( $N_{\text{SVD}}$ ) with respect to the exact (uncompressed) CCSDT method (cc-pVTZ basis set). The results are given for the molecules: methane (upper left panel), ethyne (upper right panel), nitrous oxide (lower left panel), and nitric acid (lower right panel). The horizontal red dashed line marks the 1 kJ/mol accuracy threshold (the chemical accuracy). The maximum possible size of the SVD space is given below each graph.

as essentially free from the density-fitting error. Of course, this problem occurs only if the total correlation energies are compared; in evaluation of relative energies the density-fitting error is known to systematically cancel out leaving only a very small residual error.

The results of benchmark calculations are represented graphically in Fig. 4 where SVD-CCSDT errors (with respect to the conventional CCSDT) are plotted against the SVD subspace size. One can see that the errors vanish rather quickly and the assumed 1 kJ/mol

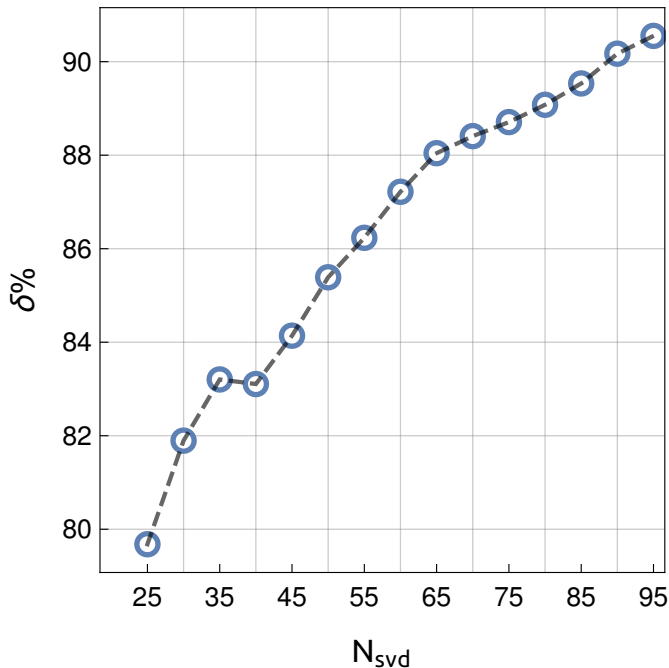


Figure 5: Accuracy of the post-CC3 energy contribution, see Eq. (40) for a precise definition, as a function of the SVD subspace size for the nitrous oxide molecule (cc-pVTZ basis set). The black dashed lines are linear functions connecting two neighbouring data points.

accuracy goal (the chemical accuracy) is reached with a small fraction of the total number of SVD vectors. The overall picture is very similar to the results reported recently at the CC3 level of theory, but we found that there appears to be no systematic relationship connecting the convergence rates of SVD-CC3 and SVD-CCSDT methods that would hold for a broader range of systems. At present, the ultimate limit of accuracy of the SVD-CCSDT method appears to be the level of  $\pm 0.1 - 0.2$  kJ/mol where oscillations start to appear. This is a consequence of increasing numerical instabilities in the procedure of obtaining consecutive SVD vectors and we hope to improve the procedures introduced in Ref. 36 to eliminate this problem in future works. Other possible strategies to increase the accuracy of the present approach are discussed in the next section. All in all, the results presented in Fig. 4 indicate that the chemical accuracy of the SVD-CCSDT energies can be reached without significant difficulties and even more stringent accuracy levels are obtainable with acceptable sizes of the SVD subspace.

From the point of view of some applications it would be beneficial to use SVD-CCSDT

method to calculate only the post-CC3 [or post-CCSD(T)] energy correction, rather than the total SVD-CCSDT result, e.g., when the uncompressed CC3 results are available (possibly calculated without the density fitting approximation). In this case the post-CC3 effects can be evaluated as a difference between SVD-CCSDT and SVD-CC3 results obtained with *the same* SVD subspace (note that the density-fitting error is cancelled out in the process). To verify whether such approach is reasonable let us define the following quantity that measures the accuracy of the calculated post-CC3 effects (on percentage basis)

$$\delta\% = 100 \left| \frac{E_{\text{SVD-CCSDT}} - E_{\text{SVD-CC3}}}{E_{\text{CCSDT}} - E_{\text{CC3}}} \right| \quad (40)$$

where  $E_{\text{SVD-CCSDT}}$ ,  $E_{\text{SVD-CC3}}$  are SVD-CCSDT and SVD-CC3 correlation energies, respectively, obtained with the same SVD subspace, and  $E_{\text{CCSDT}}$  and  $E_{\text{CC3}}$  are the conventional CCSDT and CC3 results. In Fig. 5 we illustrate the dependence of  $\delta\%$  on the size of the SVD subspace for the the nitrous oxide molecule in the cc-pVTZ basis set. Even a very small number of SVD vectors allows to recover about 80% of the total post-CC3 effects. To reproduce about 90% of the exact value a somewhat larger SVD subspace is required, corresponding to  $\rho \approx 15\%$ . A systematic convergence pattern towards the exact value is also notable, but it is not necessarily the same as for the raw energies since SVD-CC3 and SVD-CCSDT components may converge at a somewhat different rate. Taking into consideration that the calculation of the post-CC3 [or post-CCSD(T)] effects is notoriously difficult, as well documented in the literature,<sup>116</sup> the method presented here becomes an interesting alternative, especially in larger basis sets and for systems where these effects are essential for achieving the chemical accuracy.

Finally let us consider calculation of relative energies with the help of SVD-CCSDT method. For this purpose we consider the 1,3-butadiene molecule which can assume several interesting geometric structures<sup>117</sup> that are distinguished by the value of the CCCC dihedral angle,  $\theta$ . The planar *trans* geometry ( $\theta = 180^\circ$ ) is the global energy minimum while the

Table 2: Mean absolute deviation and maximum deviation (both in kJ/mol) of the SVD-CCSDT results from the corresponding uncompressed CCSDT values for torsional energy in butadiene molecule (cc-pVDZ basis set). The data set consists of eighteen CCCC dihedral angles,  $\theta = 0, 10, 20, \dots, 170$ .

$N_{\text{SVD}}$	$\rho$	mean abs. deviation	maximum deviation
20	2.6	0.92	2.10
40	5.1	0.77	1.61
60	7.7	0.42	1.02
80	10.2	0.27	0.73
100	12.8	0.19	0.50
120	15.4	0.14	0.30

analogous *cis* structure ( $\theta = 0^\circ$ ) is a saddle point on the potential energy surface. Interestingly, there is another stable conformer – the so-called *gauche* structure that appears for the dihedral angle  $\theta \approx 35^\circ$  and represents a local minimum. The *gauche* and *trans* structures are separated by a large energy barrier with a maximum for  $\theta \approx 100^\circ$ .

We performed SVD-CCSDT calculations for the butadiene molecule (cc-pVDZ basis set) for the dihedral angles  $\theta = 0, 10, 20, \dots, 180^\circ$  with the rest of the geometry being the same as in the *trans* conformer. In Table 2 we report mean absolute deviation and maximum deviation of the SVD-CCSDT torsional energies from the corresponding uncompressed CCSDT values for  $\theta = 0, 10, 20, \dots, 170^\circ$  and  $N_{\text{SVD}} = 20, 40, \dots, 120$ . All results were arranged so that the *trans* structure ( $\theta = 180^\circ$ ) corresponds to zero energy level and is thus excluded from the error statistics. The results are also presented graphically in Fig. 6 where torsional energy curve and errors with respect to CCSDT are shown for each individual point. It is clear that even small SVD subspaces provide results that are close to the chemical accuracy. With  $N_{\text{SVD}} = 60$  ( $\rho \approx 7.7\%$ ) all data points are already accurate to 1 kJ/mol or better, and  $N_{\text{SVD}} = 120$  ( $\rho \approx 15.4\%$ ) gives results that, on average, are accurate to about 0.1 kJ/mol. The errors shown in Fig. 6 exhibit a regular and predictable behaviour without major jumps and discontinuities, and there is only one minor exception occurring for  $N_{\text{SVD}} = 80$  around

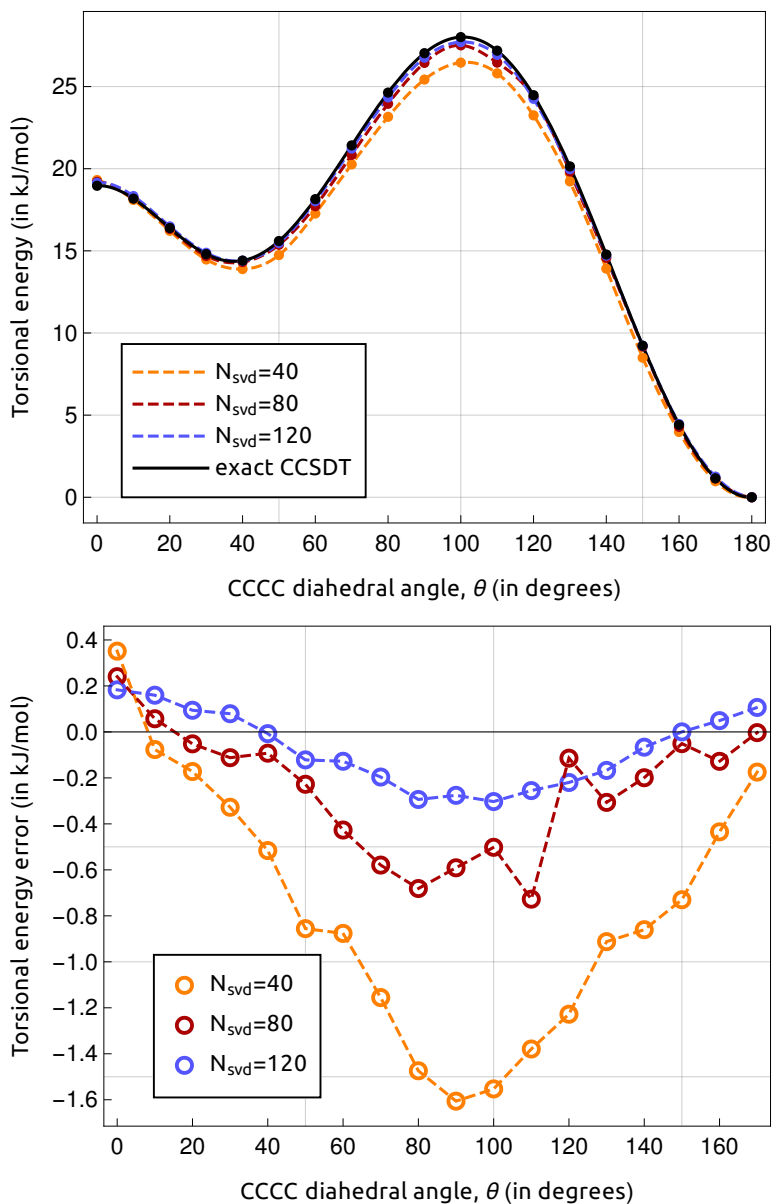


Figure 6: Torsional energy curve (upper panel) and torsional energy errors (lower panel) with respect to the exact CCSDT results calculated with the SVD-CCSDT method with  $N_{\text{SVD}} = 40, 80, 120$  for butadiene molecule. The maximum size of the SVD subspace is 781.

$\theta = 120^\circ$ .

Comparison with analogous data obtained for the total energies leads to a conclusion that a systematic cancellation of errors occurs in the evaluation of relative SVD-CCSDT energies, thereby making the compressed coupled-cluster method even more beneficial under such circumstances. This is especially true for smaller SVD subspaces. Moreover, this



Table 3: Parameters of the torsional energy curve (see text) for butadiene molecule determined with SVD-CCSDT and the uncompressed CCSDT methods (cc-pVDZ basis set). The energies are given in kJ/mol and angles in degrees.

parameter	$N_{\text{SVD}}$			exact CCSDT
	40	80	120	
$\theta_{\text{gauche}}$	39.4	37.6	37.6	37.6
$\theta_{\text{max}}$	101.5	99.6	100.7	100.6
$\Delta E_{\text{barier}}$	26.5	27.5	27.8	28.0
$\Delta E_{\text{gauche/trans}}$	13.9	14.3	14.4	14.4
$\Delta E_{\text{cis/trans}}$	19.3	19.2	19.1	19.0

example shows that the errors resulting from the truncation of the SVD subspace are weakly dependent on the geometry of the molecule provided that the same SVD subspace size is used consistently for all data points. This property is critical in computation of potentially surfaces that are smooth and regular, and thus can be fitted with a suitably chosen analytic functional form in order to, e.g., generate the molecular rotational/vibrational spectra or perform nuclear dynamics simulations.

Lastly we assess the accuracy of some parameters that characterize the calculated torsional energy curve. These are:

- values of the dihedral angle corresponding to the gauche structure ( $\theta_{\text{gauche}}$ ) and the maximum of the barrier ( $\theta_{\text{max}}$ );
- the height of the barrier with respect to the trans structure ( $\Delta E_{\text{barier}}$ );
- the energy difference between the gauche and trans structures ( $\Delta E_{\text{gauche/trans}}$ ) and between the cis and trans structures ( $\Delta E_{\text{cis/trans}}$ ).

For each method the above values were determined numerically with the help of  $B$ -splines interpolation of the calculated relative energies ( $\theta = 0, 10, 20, \dots, 180^\circ$ ). The results for  $N_{\text{SVD}} = 40, 80, 120$  are shown in Table 3. Already for  $N_{\text{SVD}} = 120$  the difference between

SVD-CCSDT and the exact CCSDT is probably smaller than the intrinsic accuracy of the latter. The obtained results agree reasonably well with the data available in the literature.<sup>117–121</sup>

## 5 Conclusions and outlook

We have reported an implementation of the full CCSDT electronic structure method using tensor decompositions to electron repulsion integrals and triple excitation amplitudes. The standard density-fitting approximation is used for the integrals while the triple amplitude tensor is represented in a Tucker-3 format. The quantities  $U_{ai}^X$  used for the expansion in Eq. (1) are obtained by performing SVD of an approximate  $t_{ijk}^{abc}$  tensor and retaining only those singular vectors that correspond to the largest singular values, as detailed previously.<sup>36</sup> The compressed tensor  $t_{XYZ}$  in Eq. (1) is obtained by performing coupled-cluster iterations within a subspace of triple excitations spanned by the chosen SVD basis.

The efficiency of this method relies on an observation that the optimal size of the SVD basis,  $N_{\text{SVD}}$ , that is sufficient to deliver a constant relative accuracy of the correlation energy grows only linearly with the size of the system. This strategy allows to reduce the computational effort significantly, and leads to an approximate CCSDT method with practically  $N^6$  scaling of its costs with the system size. This fact has been demonstrated by performing SVD-CCSDT calculations for linear alkanes with increasing chain length and analysing the computational timings.

The accuracy of the proposed method has been assessed by comparison with the exact (uncompressed) CCSDT. In the case of total energies it has been shown that for several small molecular systems the compression rates  $\rho < 20\%$  are more than sufficient to get chemically-accurate results. Taking into consideration that the compression rate  $\rho$  is (asymptotically) inversely proportional to the size of the system, these results are very promising. In the case of relative energies we have observed a significant systematic cancellation of errors making

accuracy levels below 1 kJ/mol achievable with a considerably smaller  $N_{\text{SVD}}$  than for the total energies. The obtained relative energies exhibit a regular and predictable behaviour, without major jumps or discontinuities. We have also found that at present the practical accuracy limit of the SVD-CCSDT method is around 0.1 kJ/mol due to oscillations caused by increasing numerical instabilities in the procedure of determining larger SVD subspaces. It is also worth pointing out that the SVD-CCSDT method preserves the appealing black-box nature of single-reference coupled-cluster theories and requires only one additional parameter ( $N_{\text{SVD}}$ ) to be specified by the user.

This work opens up a window for new developments in the field of “compressed” coupled-cluster theory. The most obvious extensions are perturbative methods that account for triple excitations outside the SVD subspace, as well as for quadruple excitations. Both types of corrections can be derived starting with the biorthogonal representation of the SVD-CCSDT state as the zeroth-order wavefunction. This formalism, related to the method-of-moments coupled-cluster theory,<sup>122</sup> was introduced by Stanton<sup>123</sup> to explain the success of CCSD(T) over other methods that account for triple excitation perturbatively. Subsequently, a similar reasoning has been employed to derive systematic perturbative corrections for higher excitations.<sup>29–31,124</sup>

Another interesting idea is solve for the so-called  $\Lambda$  amplitudes<sup>125–128</sup> and evaluate the first-order properties such as multipole moments, nuclear gradients or electronic densities, from the coupled-cluster functional. Since in the CCSDT method  $\Lambda$  and  $T^\dagger$  are identical in the leading-order of perturbation theory, one can expect the SVD subspace used for  $T$  to be adequate also for the expansion of  $\Lambda$ . Application of the present tensor decomposition formalism to excited-state wavefunctions *via* the equation-of-motion theory<sup>129–132</sup> is also interesting due to capability of treating, e.g., doubly excited states. However, this is more complicated than computation of properties since determination of a proper SVD subspace requires to target one state at a time.

## Acknowledgement

I would like to thank Dr. A. Tucholska and Prof. B. Jeziorski for fruitful discussions, and for reading and commenting on the manuscript. This work was supported by the National Science Center, Poland within the project 2017/27/B/ST4/02739.

## Supporting Information Available

The following files are available free of charge. The following files are available free of charge:

- **supp.pdf**: geometries of all molecules used as test cases in this work (XYZ or ZMAT formats).

## References

- (1) Coester, F. Bound states of a many-particle system. *Nuc. Phys.* **1958**, *7*, 421 – 424.
- (2) Coester, F.; Kümmel, H. Short-range correlations in nuclear wave functions. *Nuc. Phys.* **1960**, *17*, 477 – 485.
- (3) Čížek, J. On the Correlation Problem in Atomic and Molecular Systems. Calculation of Wavefunction Components in Ursell-Type Expansion Using Quantum-Field Theoretical Methods. *J. Chem. Phys.* **1966**, *45*, 4256–4266.
- (4) Čížek, J. On the Use of the Cluster Expansion and the Technique of Diagrams in Calculations of Correlation Effects in Atoms and Molecules. *Adv. Chem. Phys.* **1966**, *14*, 35–89.
- (5) Čížek, J.; Paldus, J. Correlation problems in atomic and molecular systems III. Rederivation of the coupled-pair many-electron theory using the traditional quantum chemical method. *Int. J. Quantum Chem.* **1971**, *5*, 359–379.

- (6) Paldus, J.; Čížek, J.; Shavitt, I. Correlation Problems in Atomic and Molecular Systems. IV. Extended Coupled-Pair Many-Electron Theory and Its Application to the  $\text{BH}_3$  Molecule. *Phys. Rev. A* **1972**, *5*, 50–67.
- (7) Crawford, T. D.; Schaefer III, H. F. An Introduction to Coupled Cluster Theory for Computational Chemists. *Rev. Comp. Chem.* **2000**, *14*, 33–136.
- (8) Bartlett, R. J.; Musiał, M. Coupled-cluster theory in quantum chemistry. *Rev. Mod. Phys.* **2007**, *79*, 291–352.
- (9) Purvis, G. D.; Bartlett, R. J. A full coupled-cluster singles and doubles model: The inclusion of disconnected triples. *J. Chem. Phys.* **1982**, *76*, 1910–1918.
- (10) Scuseria, G. E.; Scheiner, A. C.; Lee, T. J.; Rice, J. E.; Schaefer, H. F. The closed-shell coupled cluster single and double excitation (CCSD) model for the description of electron correlation. A comparison with configuration interaction (CISD) results. *J. Chem. Phys.* **1987**, *86*, 2881–2890.
- (11) Raghavachari, K.; Trucks, G. W.; Pople, J. A.; Head-Gordon, M. A fifth-order perturbation comparison of electron correlation theories. *Chem. Phys. Lett.* **1989**, *157*, 479–483.
- (12) Császár, A. G.; Allen, W. D.; Schaefer, H. F. In pursuit of the ab initio limit for conformational energy prototypes. *J. Chem. Phys.* **1998**, *108*, 9751–9764.
- (13) Halkier, A.; Larsen, H.; Olsen, J.; Jørgensen, P.; Gauss, J. Full configuration interaction benchmark calculations of first-order one-electron properties of BH and HF. *J. Chem. Phys.* **1999**, *110*, 734–740.
- (14) Sordo, J. A. Performance of CCSDT for first row AB/AB<sup>-</sup> diatomics: Dissociation energies and electron affinities. *J. Chem. Phys.* **2001**, *114*, 1974–1980.

- (15) Harding, M. E.; Gauss, J.; Pflüger, K.; Werner, H.-J. High-Accuracy Extrapolated Ab Initio Thermochemistry of Vinyl Chloride. *J. Phys. Chem. A* **2007**, *111*, 13623–13628.
- (16) Vázquez, J.; Harding, M. E.; Gauss, J.; Stanton, J. F. High-Accuracy Extrapolated ab Initio Thermochemistry of the Propargyl Radical and the Singlet C<sub>3</sub>H<sub>2</sub> Carbenes. *J. Phys. Chem. A* **2009**, *113*, 12447–12453.
- (17) Feller, D.; Peterson, K. A. High level coupled cluster determination of the structure, frequencies, and heat of formation of water. *J. Chem. Phys.* **2009**, *131*, 154306.
- (18) Chandrasekher, C. A.; Griffith, K. S.; Gellene, G. I. Symmetry breaking and electron correlation in O<sub>2</sub><sup>+</sup>, O<sub>2</sub>, and O<sub>2</sub><sup>-</sup>: A comparison of coupled cluster and quadratic configuration interaction approaches. *Int. J. Quantum Chem.* **1996**, *58*, 29–39.
- (19) Laidig, W. D.; Saxe, P.; Bartlett, R. J. The description of N<sub>2</sub> and F<sub>2</sub> potential energy surfaces using multireference coupled cluster theory. *J. Chem. Phys.* **1987**, *86*, 887–907.
- (20) Kowalski, K.; Piecuch, P. The method of moments of coupled-cluster equations and the renormalized CCSD[T], CCSD(T), CCSD(TQ), and CCSDT(Q) approaches. *J. Chem. Phys.* **2000**, *113*, 18–35.
- (21) Piecuch, P.; Kowalski, K.; Pimienta, I. S. O.; McGuire, M. J. Recent advances in electronic structure theory: Method of moments of coupled-cluster equations and renormalized coupled-cluster approaches. *Int. Rev. Phys. Chem.* **2002**, *21*, 527–655.
- (22) Piecuch, P.; Kowalski, K.; Pimienta, I. S. O.; Fan, P.-D.; Lodriguito, M.; McGuire, M. J.; Kucharski, S. A.; Kuś, T.; Musiał, M. Method of moments of coupled-cluster equations: a new formalism for designing accurate electronic structure methods for ground and excited states. *Theor. Chem. Acc.* **2004**, *112*, 349–393.

- (23) Shen, J.; Piecuch, P. Biorthogonal moment expansions in coupled-cluster theory: Review of key concepts and merging the renormalized and active-space coupled-cluster methods. *Chem. Phys.* **2012**, *401*, 180–202, cited By 45.
- (24) Noga, J.; Bartlett, R. J. The full CCSDT model for molecular electronic structure. *J. Chem. Phys.* **1987**, *86*, 7041–7050.
- (25) Scuseria, G. E.; Schaefer, H. F. A new implementation of the full CCSDT model for molecular electronic structure. *Chem. Phys. Lett.* **1988**, *152*, 382 – 386.
- (26) Kucharski, S. A.; Bartlett, R. J. Coupled-cluster methods that include connected quadruple excitations,  $T_4$ : CCSDTQ-1 and Q(CCSDT). *Chem. Phys. Lett.* **1989**, *158*, 550 – 555.
- (27) Kucharski, S. A.; Bartlett, R. J. An efficient way to include connected quadruple contributions into the coupled cluster method. *J. Chem. Phys.* **1998**, *108*, 9221–9226.
- (28) Kucharski, S. A.; Kolaski, M.; Bartlett, R. J. Toward the limits of predictive electronic structure theory: Connected quadruple excitations for large basis set calculations. *J. Chem. Phys.* **2001**, *114*, 692–700.
- (29) Bomble, Y. J.; Stanton, J. F.; Kállay, M.; Gauss, J. Coupled-cluster methods including noniterative corrections for quadruple excitations. *J. Chem. Phys.* **2005**, *123*, 054101.
- (30) Kállay, M.; Gauss, J. Approximate treatment of higher excitations in coupled-cluster theory. *J. Chem. Phys.* **2005**, *123*, 214105.
- (31) Kállay, M.; Gauss, J. Approximate treatment of higher excitations in coupled-cluster theory. II. Extension to general single-determinant reference functions and improved approaches for the canonical Hartree-Fock case. *J. Chem. Phys.* **2008**, *129*, 144101.
- (32) Tucker, L. R. Some mathematical notes on three-mode factor analysis. *Psychometrika* **1966**, *31*, 279–311.

- (33) Hino, O.; Kinoshita, T.; Bartlett, R. J. Singular value decomposition applied to the compression of  $T_3$  amplitude for the coupled cluster method. *J. Chem. Phys.* **2004**, *121*, 1206–1213.
- (34) Lee, Y. S.; Kucharski, S. A.; Bartlett, R. J. A coupled cluster approach with triple excitations. *J. Chem. Phys.* **1984**, *81*, 5906–5912.
- (35) Noga, J.; Bartlett, R. J.; Urban, M. Towards a full CCSDT model for electron correlation. CCSDT-n models. *Chem. Phys. Lett.* **1987**, *134*, 126 – 132.
- (36) Lesiuk, M. Efficient singular-value decomposition of the coupled-cluster triple excitation amplitudes. *J. Comp. Chem.* **2019**, *40*, 1319–1332.
- (37) Kinoshita, T.; Hino, O.; Bartlett, R. J. Singular value decomposition approach for the approximate coupled-cluster method. *J. Chem. Phys.* **2003**, *119*, 7756–7762.
- (38) Benedikt, U.; Böhm, K.-H.; Auer, A. A. Tensor decomposition in post-Hartree-Fock methods. II. CCD implementation. *J. Chem. Phys.* **2013**, *139*, 224101.
- (39) Parrish, R. M.; Zhao, Y.; Hohenstein, E. G.; Martínez, T. J. Rank reduced coupled cluster theory. I. Ground state energies and wavefunctions. *J. Chem. Phys.* **2019**, *150*, 164118.
- (40) Whitten, J. L. Coulombic potential energy integrals and approximations. *J. Chem. Phys.* **1973**, *58*, 4496–4501.
- (41) Dunlap, B. I.; Connolly, J. W. D.; Sabin, J. R. On some approximations in applications of  $X\alpha$  theory. *J. Chem. Phys.* **1979**, *71*, 3396–3402.
- (42) Vahtras, O.; Almlöf, J.; Feyereisen, M. Integral approximations for LCAO-SCF calculations. *Chem. Phys. Lett.* **1993**, *213*, 514 – 518.



- (43) Feyereisen, M.; Fitzgerald, G.; Komornicki, A. Use of approximate integrals in ab initio theory. An application in MP2 energy calculations. *Chem. Phys. Lett.* **1993**, *208*, 359 – 363.
- (44) Rendell, A. P.; Lee, T. J. Coupled-cluster theory employing approximate integrals: An approach to avoid the input/output and storage bottlenecks. *J. Chem. Phys.* **1994**, *101*, 400–408.
- (45) Kendall, R. A.; Früchtl, H. A. The impact of the resolution of the identity approximate integral method on modern ab initio algorithm development. *Theor. Chem. Acc.* **1997**, *97*, 158–163.
- (46) Weigend, F. A fully direct RI-HF algorithm: Implementation, optimised auxiliary basis sets, demonstration of accuracy and efficiency. *Phys. Chem. Chem. Phys.* **2002**, *4*, 4285–4291.
- (47) Epifanovsky, E.; Zuev, D.; Feng, X.; Khistyayev, K.; Shao, Y.; Krylov, A. I. General implementation of the resolution-of-the-identity and Cholesky representations of electron repulsion integrals within coupled-cluster and equation-of-motion methods: Theory and benchmarks. *J. Chem. Phys.* **2013**, *139*, 134105.
- (48) DePrince, A. E.; Sherrill, C. D. Accuracy and Efficiency of Coupled-Cluster Theory Using Density Fitting/Cholesky Decomposition, Frozen Natural Orbitals, and a t1-Transformed Hamiltonian. *J. Chem. Theory Comp.* **2013**, *9*, 2687–2696.
- (49) Eugene DePrince, I.; Kennedy, M. R.; Sumpter, B. G.; Sherrill, C. D. Density-fitted singles and doubles coupled cluster on graphics processing units. *Mol. Phys.* **2014**, *112*, 844–852.
- (50) Beebe, N. H. F.; Linderberg, J. Simplifications in the generation and transformation of two-electron integrals in molecular calculations. *Int. J. Quantum Chem.* **1997**, *12*, 683–705.

- (51) Røeggen, I.; Wisløff-Nilssen, E. On the Beebe-Linderberg two-electron integral approximation. *Chem. Phys. Lett.* **1986**, *132*, 154 – 160.
- (52) Koch, H.; Sánchez de Merás, A.; Pedersen, T. B. Reduced scaling in electronic structure calculations using Cholesky decompositions. *J. Chem. Phys.* **2003**, *118*, 9481–9484.
- (53) Aquilante, F.; Pedersen, T. B.; Lindh, R. Low-cost evaluation of the exchange Fock matrix from Cholesky and density fitting representations of the electron repulsion integrals. *J. Chem. Phys.* **2007**, *126*, 194106.
- (54) Aquilante, F.; Gagliardi, L.; Pedersen, T. B.; Lindh, R. Atomic Cholesky decompositions: A route to unbiased auxiliary basis sets for density fitting approximation with tunable accuracy and efficiency. *J. Chem. Phys.* **2009**, *130*, 154107.
- (55) Friesner, R. A. Solution of self-consistent field electronic structure equations by a pseudospectral method. *Chem. Phys. Lett.* **1985**, *116*, 39 – 43.
- (56) Friesner, R. A. Solution of the Hartree-Fock equations by a pseudospectral method: Application to diatomic molecules. *J. Chem. Phys.* **1986**, *85*, 1462–1468.
- (57) Friesner, R. A. Solution of the Hartree-Fock equations for polyatomic molecules by a pseudospectral method. *J. Chem. Phys.* **1987**, *86*, 3522–3531.
- (58) Friesner, R. A. An automatic grid generation scheme for pseudospectral self-consistent field calculations on polyatomic molecules. *J. Phys. Chem.* **1988**, *92*, 3091–3096.
- (59) Ringnalda, M. N.; Won, Y.; Friesner, R. A. Pseudospectral Hartree-Fock calculations on glycine. *J. Chem. Phys.* **1990**, *92*, 1163–1173.
- (60) Ringnalda, M. N.; Belhadj, M.; Friesner, R. A. Pseudospectral Hartree-Fock theory: Applications and algorithmic improvements. *J. Chem. Phys.* **1990**, *93*, 3397–3407.

- (61) Greeley, B. H.; Russo, T. V.; Mainz, D. T.; Friesner, R. A.; Langlois, J.; Goddard, W. A.; Donnelly, R. E.; Ringnalda, M. N. New pseudospectral algorithms for electronic structure calculations: Length scale separation and analytical two-electron integral corrections. *J. Chem. Phys.* **1994**, *101*, 4028–4041.
- (62) Friesner, R. A.; Murphy, R. B.; Beachy, M. D.; Ringnalda, M. N.; Pollard, W. T.; Dunietz, B. D.; Cao, Y. Correlated ab Initio Electronic Structure Calculations for Large Molecules. *J. Phys. Chem. A* **1999**, *103*, 1913–1928.
- (63) Neese, F.; Wennmohs, F.; Hansen, A.; Becker, U. Efficient, approximate and parallel Hartree-Fock and hybrid DFT calculations. A 'chain-of-spheres' algorithm for the Hartree-Fock exchange. *Chem. Phys.* **2009**, *356*, 98 – 109.
- (64) Kossmann, S.; Neese, F. Efficient Structure Optimization with Second-Order Many-Body Perturbation Theory: The RIJCOSX-MP2 Method. *J. Chem. Theory Comput.* **2010**, *6*, 2325–2338.
- (65) Izsák, R.; Neese, F. An overlap fitted chain of spheres exchange method. *J. Chem. Phys.* **2011**, *135*, 144105.
- (66) Petrenko, T.; Kossmann, S.; Neese, F. Efficient time-dependent density functional theory approximations for hybrid density functionals: Analytical gradients and parallelization. *J. Chem. Phys.* **2011**, *134*, 054116.
- (67) Izsák, R.; Hansen, A.; Neese, F. The resolution of identity and chain of spheres approximations for the LPNO-CCSD singles Fock term. *Mol. Phys.* **2012**, *110*, 2413–2417.
- (68) Izsák, R.; Neese, F. Speeding up spin-component-scaled third-order perturbation theory with the chain of spheres approximation: the COSX-SCS-MP3 method. *Mol. Phys.* **2013**, *111*, 1190–1195.

- (69) Dutta, A. K.; Neese, F.; Izsák, R. Speeding up equation of motion coupled cluster theory with the chain of spheres approximation. *J. Chem. Phys.* **2016**, *144*, 034102.
- (70) Hohenstein, E. G.; Parrish, R. M.; Martínez, T. J. Tensor hypercontraction density fitting. I. Quartic scaling second- and third-order Møller-Plesset perturbation theory. *J. Chem. Phys.* **2012**, *137*, 044103.
- (71) Parrish, R. M.; Hohenstein, E. G.; Martínez, T. J.; Sherrill, C. D. Tensor hypercontraction. II. Least-squares renormalization. *J. Chem. Phys.* **2012**, *137*, 224106.
- (72) Parrish, R. M.; Hohenstein, E. G.; Schunck, N. F.; Sherrill, C. D.; Martínez, T. J. Exact Tensor Hypercontraction: A Universal Technique for the Resolution of Matrix Elements of Local Finite-Range  $N$ -Body Potentials in Many-Body Quantum Problems. *Phys. Rev. Lett.* **2013**, *111*, 132505.
- (73) Benedikt, U.; Auer, A. A.; Espig, M.; Hackbusch, W. Tensor decomposition in post-Hartree-Fock methods. I. Two-electron integrals and MP2. *J. Chem. Phys.* **2011**, *134*, 054118.
- (74) Almlöf, J. Elimination of energy denominators in Møller-Plesset perturbation theory by a Laplace transform approach. *Chem. Phys. Lett.* **1991**, *181*, 319 – 320.
- (75) Jung, Y.; Lochan, R. C.; Dutoi, A. D.; Head-Gordon, M. Scaled opposite-spin second order Møller-Plesset correlation energy: An economical electronic structure method. *J. Chem. Phys.* **2004**, *121*, 9793–9802.
- (76) Aquilante, F.; Pedersen, T. B. Quartic scaling evaluation of canonical scaled opposite spin second-order Møller-Plesset correlation energy using Cholesky decompositions. *Chem. Phys. Lett.* **2007**, *449*, 354 – 357.
- (77) Kokkila Schumacher, S. I. L.; Hohenstein, E. G.; Parrish, R. M.; Wang, L.-P.; Martínez, T. J. Tensor Hypercontraction Second-Order Møller-Plesset Perturbation

- Theory: Grid Optimization and Reaction Energies. *J. Chem. Theory Comput.* **2015**, *11*, 3042–3052.
- (78) Song, C.; Martínez, T. J. Atomic orbital-based SOS-MP2 with tensor hypercontraction. II. Local tensor hypercontraction. *J. Chem. Phys.* **2017**, *146*, 034104.
- (79) Hohenstein, E. G.; Parrish, R. M.; Sherrill, C. D.; Martínez, T. J. Communication: Tensor hypercontraction. III. Least-squares tensor hypercontraction for the determination of correlated wavefunctions. *J. Chem. Phys.* **2012**, *137*, 221101.
- (80) Schutski, R.; Zhao, J.; Henderson, T. M.; Scuseria, G. E. Tensor-structured coupled cluster theory. *J. Chem. Phys.* **2017**, *147*, 184113.
- (81) Adamowicz, L.; Bartlett, R. J. Optimized virtual orbital space for high-level correlated calculations. *J. Chem. Phys.* **1987**, *86*, 6314–6324.
- (82) Adamowicz, L.; Bartlett, R. J.; Sadlej, A. J. Optimized virtual orbital space for high-level correlated calculations. II. Electric properties. *J. Chem. Phys.* **1988**, *88*, 5749–5758.
- (83) Neogrady, P.; Pitoňák, M.; Urban, M. Optimized virtual orbitals for correlated calculations: an alternative approach. *Mol. Phys.* **2005**, *103*, 2141–2157.
- (84) Pitoňák, M.; Holka, F.; Neogrady, P.; Urban, M. Optimized virtual orbitals for correlated calculations: Towards large scale CCSD(T) calculations of molecular dipole moments and polarizabilities. *J. Mol. Struct.* **2006**, *768*, 79 – 89.
- (85) Sosa, C.; Geertsen, J.; Trucks, G. W.; Bartlett, R. J.; Franz, J. A. Selection of the reduced virtual space for correlated calculations. An application to the energy and dipole moment of H<sub>2</sub>O. *Chem. Phys. Lett.* **1989**, *159*, 148 – 154.
- (86) Taube, A. G.; Bartlett, R. J. Frozen Natural Orbitals: Systematic Basis Set Truncation for Coupled-Cluster Theory. *Collect. Czech. Chem. Commun.* **2006**, *70*, 837–850.

- (87) Taube, A. G.; Bartlett, R. J. Frozen natural orbital coupled-cluster theory: Forces and application to decomposition of nitroethane. *J. Chem. Phys.* **2008**, *128*, 164101.
- (88) Yang, J.; Kurashige, Y.; Manby, F. R.; Chan, G. K. L. Tensor factorizations of local second-order Møller-Plesset theory. *J. Chem. Phys.* **2011**, *134*, 044123.
- (89) Kurashige, Y.; Yang, J.; Chan, G. K.-L.; Manby, F. R. Optimization of orbital-specific virtuals in local Møller-Plesset perturbation theory. *J. Chem. Phys.* **2012**, *136*, 124106.
- (90) Yang, J.; Chan, G. K.-L.; Manby, F. R.; Schütz, M.; Werner, H.-J. The orbital-specific-virtual local coupled cluster singles and doubles method. *J. Chem. Phys.* **2012**, *136*, 144105.
- (91) Schütz, M.; Yang, J.; Chan, G. K.-L.; Manby, F. R.; Werner, H.-J. The orbital-specific virtual local triples correction: OSV-L(T). *J. Chem. Phys.* **2013**, *138*, 054109.
- (92) Neese, F.; Wennmohs, F.; Hansen, A. Efficient and accurate local approximations to coupled-electron pair approaches: An attempt to revive the pair natural orbital method. *J. Chem. Phys.* **2009**, *130*, 114108.
- (93) Riplinger, C.; Neese, F. An efficient and near linear scaling pair natural orbital based local coupled cluster method. *J. Chem. Phys.* **2013**, *138*, 034106.
- (94) Riplinger, C.; Sandhoefer, B.; Hansen, A.; Neese, F. Natural triple excitations in local coupled cluster calculations with pair natural orbitals. *J. Chem. Phys.* **2013**, *139*, 134101.
- (95) Liakos, D. G.; Sparta, M.; Kesharwani, M. K.; Martin, J. M. L.; Neese, F. Exploring the Accuracy Limits of Local Pair Natural Orbital Coupled-Cluster Theory. *J. Chem. Theory Comput.* **2015**, *11*, 1525–1539.
- (96) Schwilk, M.; Ma, Q.; Köppl, C.; Werner, H.-J. Scalable Electron Correlation Methods.

3. Efficient and Accurate Parallel Local Coupled Cluster with Pair Natural Orbitals (PNO-LCCSD). *J. Chem. Theory Comput.* **2017**, *13*, 3650–3675.
- (97) Koch, H.; Christiansen, O.; Kobayashi, R.; Jørgensen, P.; Helgaker, T. A direct atomic orbital driven implementation of the coupled cluster singles and doubles (CCSD) model. *Chem. Phys. Lett.* **1994**, *228*, 233 – 238.
- (98) Koch, H.; Sánchez de Merás, A.; Helgaker, T.; Christiansen, O. The integral-direct coupled cluster singles and doubles model. *J. Chem. Phys.* **1996**, *104*, 4157–4165.
- (99) Katouda, M.; Nagase, S. Efficient parallel algorithm of second-order Møller-Plesset perturbation theory with resolution-of-identity approximation (RI-MP2). *Int. J. Quantum Chem.* **2009**, *109*, 2121–2130.
- (100) Koch, H.; Christiansen, O.; Jørgensen, P.; Sanchez de Merás, A. M.; Helgaker, T. The CC3 model: An iterative coupled cluster approach including connected triples. *J. Chem. Phys.* **1997**, *106*, 1808–1818.
- (101) Golub, G.; Kahan, W. Calculating the Singular Values and Pseudo-Inverse of a Matrix. *SIAM J. Numer. Anal.* **1965**, *2*, 205–224.
- (102) Pulay, P. Convergence acceleration of iterative sequences. the case of scf iteration. *Chem. Phys. Lett.* **1980**, *73*, 393 – 398.
- (103) Scuseria, G. E.; Lee, T. J.; Schaefer, H. F. Accelerating the convergence of the coupled-cluster approach: The use of the DIIS method. *Chem. Phys. Lett.* **1986**, *130*, 236 – 239.
- (104) Purvis, G. D.; Bartlett, R. J. The reduced linear equation method in coupled cluster theory. *J. Chem. Phys.* **1981**, *75*, 1284–1292.
- (105) Ziólkowski, M.; Weijo, V.; Jørgensen, P.; Olsen, J. An efficient algorithm for solving

- nonlinear equations with a minimal number of trial vectors: Applications to atomic-orbital based coupled-cluster theory. *J. Chem. Phys.* **2008**, *128*, 204105.
- (106) Ettenhuber, P.; Jørgensen, P. Discarding Information from Previous Iterations in an Optimal Way To Solve the Coupled Cluster Amplitude Equations. *J. Chem. Theory Comput.* **2015**, *11*, 1518–1524.
- (107) Lesiuk, M. WICKTORY – program for manipulation of second-quantized expressions and the resulting tensor products. *unpublished* **2019**,
- (108) Dunning, T. H. Gaussian basis sets for use in correlated molecular calculations. I. The atoms boron through neon and hydrogen. *J. Chem. Phys.* **1989**, *90*, 1007–1023.
- (109) Weigend, F.; Häser, M.; Patzelt, H.; Ahlrichs, R. RI-MP2: optimized auxiliary basis sets and demonstration of efficiency. *Chem. Phys. Lett.* **1998**, *294*, 143 – 152.
- (110) Schmidt, M. W.; Baldridge, K. K.; Boatz, J. A.; Elbert, S. T.; Gordon, M. S.; Jensen, J. H.; Koseki, S.; Matsunaga, N.; Nguyen, K. A.; Su, S.; Windus, T. L.; Dupuis, M.; Montgomery, J. A. General atomic and molecular electronic structure system. *J. Comp. Chem.* **1993**, *14*, 1347–1363.
- (111) Becke, A. D. Density-functional thermochemistry. I. The effect of the exchange-only gradient correction. *J. Chem. Phys.* **1992**, *96*, 2155–2160.
- (112) Stephens, P. J.; Devlin, F. J.; Chabalowski, C. F.; Frisch, M. J. Ab Initio Calculation of Vibrational Absorption and Circular Dichroism Spectra Using Density Functional Force Fields. *J. Phys. Chem.* **1994**, *98*, 11623–11627.
- (113) Hertwig, R. H.; Koch, W. On the parameterization of the local correlation functional. What is Becke-3-LYP? *Chem. Phys. Lett.* **1997**, *268*, 345 – 351.
- (114) Prochnow, E.; Harding, M. E.; Gauss, J. Parallel Calculation of CCSDT and Mk-MRCCSDT Energies. *J. Chem. Theory Comput.* **2010**, *6*, 2339–2347.



- (115) Schuchardt, K. L.; Didier, B. T.; Elsethagen, T.; Sun, L.; Gurumoorthi, V.; Chase, J.; Li, J.; Windus, T. L. Basis Set Exchange: A Community Database for Computational Sciences. *J. Chem. Inf. Model* **2007**, *47*, 1045–1052.
- (116) Smith, D. G. A.; Jankowski, P.; Slawik, M.; Witek, H. A.; Patkowski, K. Basis Set Convergence of the Post-CCSD(T) Contribution to Noncovalent Interaction Energies. *J. Chem. Theory Comput.* **2014**, *10*, 3140–3150.
- (117) Feller, D.; Craig, N. C. High Level ab Initio Energies and Structures for the Rotamers of 1,3-Butadiene. *J. Phys. Chem. A* **2009**, *113*, 1601–1607.
- (118) Engeln, R.; Consalvo, D.; Reuss, J. Evidence for a gauche minor conformer of 1,3-butadiene. *Chem. Phys.* **1992**, *160*, 427 – 433.
- (119) Murcko, M. A.; Castejon, H.; Wiberg, K. B. Carbon-Carbon Rotational Barriers in Butane, 1-Butene, and 1,3-Butadiene. *J. Phys. Chem.* **1996**, *100*, 16162–16168.
- (120) c. Sancho-García, J.; Pérez-Jiménez, A. J.; Pérez-Jordá, J. M.; Moscardó, F. Torsional potential of 1,3-butadiene: ab initio calculations. *Mol. Phys.* **2001**, *99*, 47–51.
- (121) Karpfen, A.; Parasuk, V. Accurate torsional potentials in conjugated systems: ab initio and density functional calculations on 1,3-butadiene and monohalogenated butadienes. *Mol. Phys.* **2004**, *102*, 819–826.
- (122) Jankowski, K.; Paldus, J.; Piecuch, P. Method of moments approach and coupled cluster theory. *Theor. Chem. Acc.* **1991**, *80*, 223–243.
- (123) Stanton, J. F. Why CCSD(T) works: a different perspective. *Chem. Phys. Lett.* **1997**, *281*, 130 – 134.
- (124) Eriksen, J.; Kristensen, K.; Kjærgaard, T.; Jørgensen, P.; Gauss, J. A Lagrangian framework for deriving triples and quadruples corrections to the CCSD energy. *J. Chem. Phys.* **2014**, *140*, 064108.

- (125) Fitzgerald, G.; Harrison, R. J.; Bartlett, R. J. Analytic energy gradients for general coupled-cluster methods and fourth-order many-body perturbation theory. *J. Chem. Phys.* **1986**, *85*, 5143–5150.
- (126) Salter, E. A.; Trucks, G. W.; Bartlett, R. J. Analytic energy derivatives in many-body methods. I. First derivatives. *J. Chem. Phys.* **1989**, *90*, 1752–1766.
- (127) Jørgensen, P.; Helgaker, T. Møller-Plesset energy derivatives. *J. Chem. Phys.* **1988**, *89*, 1560–1570.
- (128) Helgaker, T.; Jørgensen, P.; Handy, N. C. A numerically stable procedure for calculating Møller-Plesset energy derivatives, derived using the theory of Lagrangians. *Theor. Chem. Acc.* **1989**, *76*, 227–245.
- (129) Sekino, H.; Bartlett, R. J. A linear response, coupled-cluster theory for excitation energy. *Int. J. Quantum Chem.* **1984**, *26*, 255–265.
- (130) Geertsen, J.; Rittby, M.; Bartlett, R. J. The equation-of-motion coupled-cluster method: Excitation energies of Be and CO. *Chem. Phys. Lett.* **1989**, *164*, 57 – 62.
- (131) Comeau, D. C.; Bartlett, R. J. The equation-of-motion coupled-cluster method. Applications to open- and closed-shell reference states. *Chem. Phys. Lett.* **1993**, *207*, 414 – 423.
- (132) Stanton, J. F.; Bartlett, R. J. The equation of motion coupled-cluster method. A systematic biorthogonal approach to molecular excitation energies, transition probabilities, and excited state properties. *J. Chem. Phys.* **1993**, *98*, 7029–7039.

# Graphical TOC Entry

